Petroleum Science 23 (2026) 3074–3090

Contents lists available at ScienceDirect

Petroleum Science

journal homepage: www.keaipublishing.com/en/journals/petroleum-science

Original Paper

Cenozoic morphological evolution of the Tanintharyi Shelf carbonate platform, Andaman Sea Basin: Implications for hydrocarbon reservoir potential

Xi-Wu Luan *, Thanuja D. Raveendrasinghe, Zi-Jie Wang, Li-Shuang Feng

College of Earth Science and Engineering, Shandong University of Science and Technology, Qingdao, 266590, Shandong, China

A R T I C L E I N F O

Article history:
Received 9 October 2024
Received in revised form
8 January 2026
Accepted 24 March 2026
Available online 27 March 2026

Edited by Xiu-Fang Hu

Keywords:
Andaman Sea Basin
Tanintharyi Shelf
Carbonate platform
Seismic geomorphology
Hydrocarbon reservoir heterogeneity

A B S T R A C T

The Tanintharyi Shelf in the Andaman Sea Basin hosts a significant yet largely underexplored Cenozoic carbonate platform with substantial hydrocarbon potential. This study utilizes an integrated analysis of high-resolution 2D and 3D seismic reflection data, well data, and regional stratigraphic information to elucidate the morphological evolution of this platform and assess its implications for hydrocarbon reservoirs. The findings reveal that the platform started in the Early Miocene as isolated patch reefs on fault-bounded structural highs, eventually evolving into an asymmetric, westward-dipping rimmed shelf. Its development was influenced by the interaction of syn-sedimentary tectonics, which created accommodation space and a paleotopography that shielded the shelf from clastic influx, along with eustatic sea-level fluctuations that caused cycles of sediment buildup, subaerial exposure (leading to karstification), and back-stepping. Ultimately, the platform was drowned and buried during the Middle to Late Miocene due to accelerated post-rift subsidence combined with increased siliciclastic input, the latter driven by the Neogene uplift of the Tibetan Plateau. The reservoir potential varies across the platform, with the highest concentrations in wave-resistant reefal margin facies and potential dolomitized zones on paleo-highs, where primary porosity was enhanced by meteoric diagenesis. However, reservoir quality is compartmentalized due to tight cementation and mud-rich intervals. The widespread presence of gas chimneys and pockmarks indicates that the platform functions both as a reservoir and a conduit for fluid migration. Therefore, this study establishes a predictive tectonostratigraphic framework, emphasizing that successful exploration in this complex environment requires high-resolution mapping of facies boundaries, diagenetic features, and fault architecture, combined with seal integrity analysis. The findings offer a new model for understanding the evolution of carbonate reservoirs in tectonically active, rift-margin settings worldwide.

1. Introduction

Carbonate platforms represent one of the most economically vital and geologically complex sedimentary systems on Earth, serving as the host for more than half of the world's conventional hydrocarbon reserves and sustaining critical marine ecological habitats (Jardine and Wilshart, 1987; Harris and Vlaswinkel, 2008; Joshi and Singh, 2019; Garland et al., 2025). Their exceptional reservoir potential stems from inherent high primary porosity and permeability in reefal, grainstone, and shoal facies, which can be further enhanced by post-depositional diagenetic processes such as karstification, dolomitization, and fracturing—features that make carbonate platforms a core target for global hydrocarbon exploration. Among Cenozoic carbonate systems, Miocene platforms stand out for their remarkable productivity, as exemplified by the Central Luconia carbonate province in the South China Sea, where large-scale reef-bank complexes have yielded giant gas and oil discoveries and have become a benchmark for understanding tropical carbonate deposition (Lü et al., 2013; Mathew et al., 2020; Bashir et al., 2021; Rankey, 2023; Henglai et al., 2024). However, the morphological evolution and reservoir architecture of carbonate platforms are governed by the intricate and non-linear interplay of multiple dynamic factors, including eustatic sea-level fluctuations, syn-depositional tectonic activity, climatic conditions, sediment supply, and biogenic productivity (Joshi and

* Corresponding author.
E-mail address: xluan@sdust.edu.cn (X.-W. Luan).
Peer review under the responsibility of China University of Petroleum (Beijing).

https://doi.org/10.1016/j.petsci.2026.03.057

Singh, 2019; Garland et al., 2025). This multi-factor coupling creates extreme spatial and temporal heterogeneity in platform geometry, facies distribution, and diagenetic modification, making the quantitative characterization and predictive modeling of carbonate platform evolution a longstanding challenge in sedimentary geology and petroleum geoscience (Joshi and Singh, 2019; Garland et al., 2025). Despite decades of research, significant gaps remain in the global understanding of carbonate platform morphological evolution, particularly in tectonically active rift-margin and back-arc basin settings. Most classic carbonate platform models are based on relatively stable passive continental margins, where tectonic influence is minimal and eustasy is the dominant control on platform growth and demise (Wilson, 1974; Bosence, 2005). In contrast, the response of carbonate platforms to intense syn-sedimentary faulting, strike-slip deformation, and rapid post-rift subsidence in active tectonic zones is poorly constrained; existing studies often lack high-resolution geophysical and well data to unravel the detailed spatiotemporal coupling between tectonic pulses and platform morphological changes.

This study aims to address key uncertainties by providing a detailed analysis of the morphological evolution of the Tanintharyi Shelf carbonate platform. By integrating high-resolution seismic reflection data with well logs and biostratigraphic information, it reconstructs the platform's architectural development throughout the Cenozoic Era. The main objectives are to characterize its seismic geomorphology and stratigraphic architecture, to trace its evolutionary stages in relation to regional tectonic and eustatic influences, and to assess the implications for potential hydrocarbon reservoir development in the Andaman Sea Basin.

2. Geological setting

The Andaman Sea Basin is a back-arc basin situated in the northeastern Indian Ocean, within the obliquely convergent margin between the Indian and Eurasian plates (Khan and Chakraborty, 2004; Curray, 2005; Ray and Radhakrishna, 2021) (Fig. 1). This tectonic environment, characterized by a megathrust caused by the subduction of the Indian Plate, has shaped the basin's complex development (Curray, 2005; Morley, 2017; Singh and Moeremans, 2017). Its geological origin dates back to the late Mesozoic, as shown by granitic intrusions into low-grade metamorphic rocks on the eastern shelf, which mark the closure of the Neo-Tethys Ocean (Curray, 2005; Gardiner et al., 2018). From the late Paleogene onward, subduction-related processes, including the formation of island arcs along the Benioff zone and accretionary ridges such as the Rakhine and Patkai ranges, along with the Andaman and Nicobar Islands, gradually isolated the Andaman Sea from the open Indian Ocean, turning it into a marginal sea (Moeremans and Singh, 2015; Singh and Moeremans, 2017; Jithin and Francis, 2020; Najman et al., 2022).

The Cenozoic development of the Andaman Sea has been shaped by highly oblique subduction, leading to a complex interaction of oceanic and continental regions (Hall, 2012; Chatterjee et al., 2013). A key geodynamic feature since the Late Miocene is the right-lateral wrench fault system bounded by the Sagaing and West Andaman faults, which formed a transtensional pull-apart basin (Xu et al., 2014; Raveendrasinghe et al., 2024) (Fig. 1). This process resulted in the creation of the Andaman back-arc spreading center during the Late Miocene or Pliocene, with features like the Alcock and Sewell rises indicating ongoing extensional activity (Raju et al., 2004; Morley and Alvey, 2015). At the same time, the Himalayan orogeny to the north supplied large amounts of clastic sediment to the basin through the Irrawaddy and Salween River systems (Ramaswamy and Rao, 2014; Ray and Radhakrishna, 2021; Morley et al., 2022) (Fig. 1).

The Oligocene–Neogene tectonic evolution shows considerable spatial and temporal variation in structural styles (Srisuriyon and Morley, 2014; Morley, 2017; Srivastava et al., 2021). The Mergui Basin experienced roughly E–W to WNW–ESE extension during the Oligocene, with its southern part entering a post-rift phase in the Early Miocene while the northern part underwent NNW–SSE transtensional deformation (Srisuriyon and Morley, 2014). Similarly, the East Andaman Basin, although mainly preserving a Neogene stratigraphic record, also reflects a history that began with early E–W extension and was later overprinted by NNW–SSE transtensional forces (Morley, 2017; Mahattanachai et al., 2021). This ongoing tectonic process can be broadly divided into three main phases: pre-rift (characterized by crustal stretching), rift (involving the fragmentation of the Burma Basin), and back-arc strike-slip (Srisuriyon and Morley, 2014). Spatially, it is historically associated with an accretionary prism in the west, a central zone of seafloor spreading, a northern area affected by transtensional rifting and large deltaic deposition, and an eastern region—including the Tanintharyi area—shaped by rifting and mixed sediment sources (Raju et al., 2004; Curray, 2005; Morley and Alvey, 2015).

Tanintharyi Shelf, located on the eastern edge of the Andaman Sea Basin and bordered by the Mergui Basin to the south and the East Andaman Basin to the west, is a vital area for research (Ramaswamy and Rao, 2014; Racey and Ridd, 2015a, 2015c) (Fig. 1). Its continental shelf features a unique two-tiered, terraced shape, with the first terrace situated at approximately 200 m deep and a shelf break near 800 m (Ramaswamy and Rao, 2014) (Fig. 1). This geomorphology, which extends southward as the Mergui Shelf, results from Eocene–Miocene eustatic changes and rapid Pliocene–Recent subsidence, making the modern shelf unusually deep (Morley and Alvey, 2015; Morley, 2017; Mahattanachai et al., 2021). The region's structural setup is strongly shaped by the NNE–SSW trending, highly active East Sagaing Fault, which marks its eastern boundary (Guo et al., 2023; Raveendrasinghe et al., 2024).

Stratigraphically, Tanintharyi Shelf, as revealed by M15-B-1 exploration well, consists of a thick Cenozoic succession that began with Oligocene to Middle Miocene deposits formed in the early Andaman back-arc basin and is topped by Late Miocene to Recent sediments of the modern pull-apart basin (Qiao et al., 2023; Jin et al., 2024; Raveendrasinghe et al., 2024) (Fig. 2). Terrigenous material, initially derived from the Malay Peninsula and later supplied by distal sediments from the Irrawaddy and Salween river systems, accumulated in shelf to upper slope environments (Racey and Ridd, 2015c; Jin et al., 2024). During the Early Miocene, the combination of fault-driven subsidence, sediment influx, and favorable conditions for biogenic production facilitated the development of the Tanintharyi Shelf carbonate platform (Qiao et al., 2023; Raveendrasinghe et al., 2024). The basement beneath the Tanintharyi Shelf is composed of Mesozoic granite associated with the Sibumasu Terrane, as observed in the M15-B-1 exploration well (Polachan and Racey, 1994; Racey and Ridd, 2015c; Gardiner et al., 2018; Morley et al., 2021). This complex geological setting, featuring rapid lateral and vertical facies changes and evolving tectonics, creates a dynamic environment (Guo et al., 2023; Raveendrasinghe et al., 2024) with significant but challenging potential for hydrocarbon platform evolution.

3. Dataset and methods

3.1. Study area

The M-15 Block, covering an area of 13,480 km^2 with water depths ranging from 15 m to 1900 m, is located in the Andaman Sea off the coast of Myanmar, bordered to the east by the major city of Yangon, to the northeast by the Indian ONGC-operated YEB

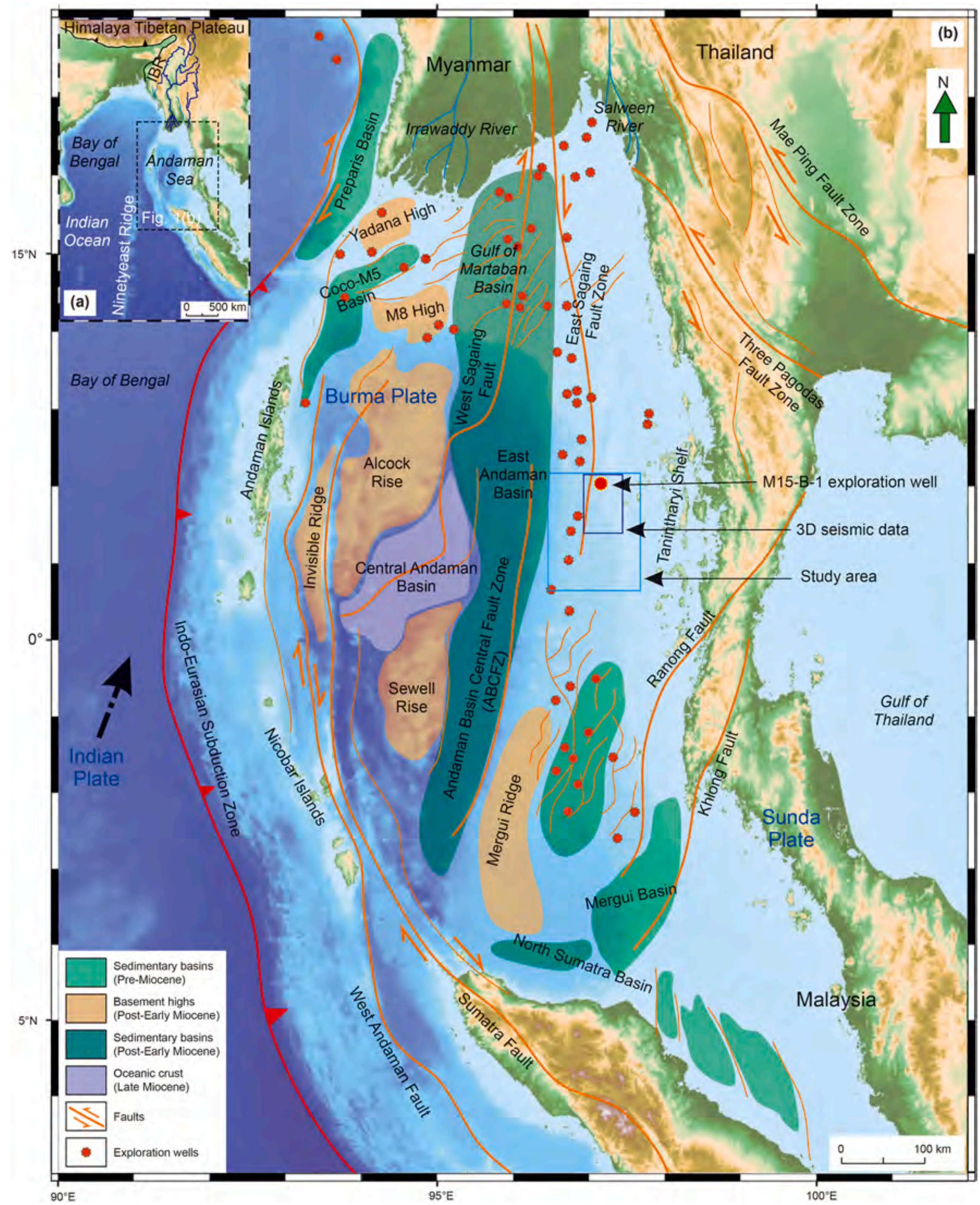

Fig. 1. **(a)** Geographical distribution of the Andaman Sea Basin in the Indian Ocean; **(b)** the spatial distribution of major sub-basins and tectonic elements of the Andaman Sea region associated with the Indo-Eurasian subduction zone, modified from Curray (2005), Morley et al. (2022), and Raveendrasinghe et al. (2024), showing the Tanintharyi Shelf study area. IBR: Indo-Burma Range.

Block, to the north by the M-14 Block containing the Yetagun Gas Field, to the northwest by the Total Energies and Eni-operated MD-4 Block, to the west by the Shell-operated MD-5 Block, and to the south by the MOGE-operated M-16 Block (Fig. 3).

3.2. Dataset

The M-15 offshore block in the Andaman Sea, Myanmar, has been covered by two distinct 3D seismic surveys to evaluate its hydrocarbon potential. In 2016, Shell plc acquired a 1500 km^2 3D seismic dataset using parameters consistent with subsequent industry standards in the region. A more extensive 5600 km^2 3D seismic survey was then executed by China National Offshore Oil Corporation (CNOOC) between February 6, 2018, and April 26, 2018, utilizing a CNOOC-operated seismic vessel. This 2018 campaign employed a marine towed-streamer 3D seismic reflection method, with a GI airgun array (4030 in^3 total volume, 7 m depth, 25 m shot interval) and 12 streamers (7050 m total length, slanted at 8–40 m

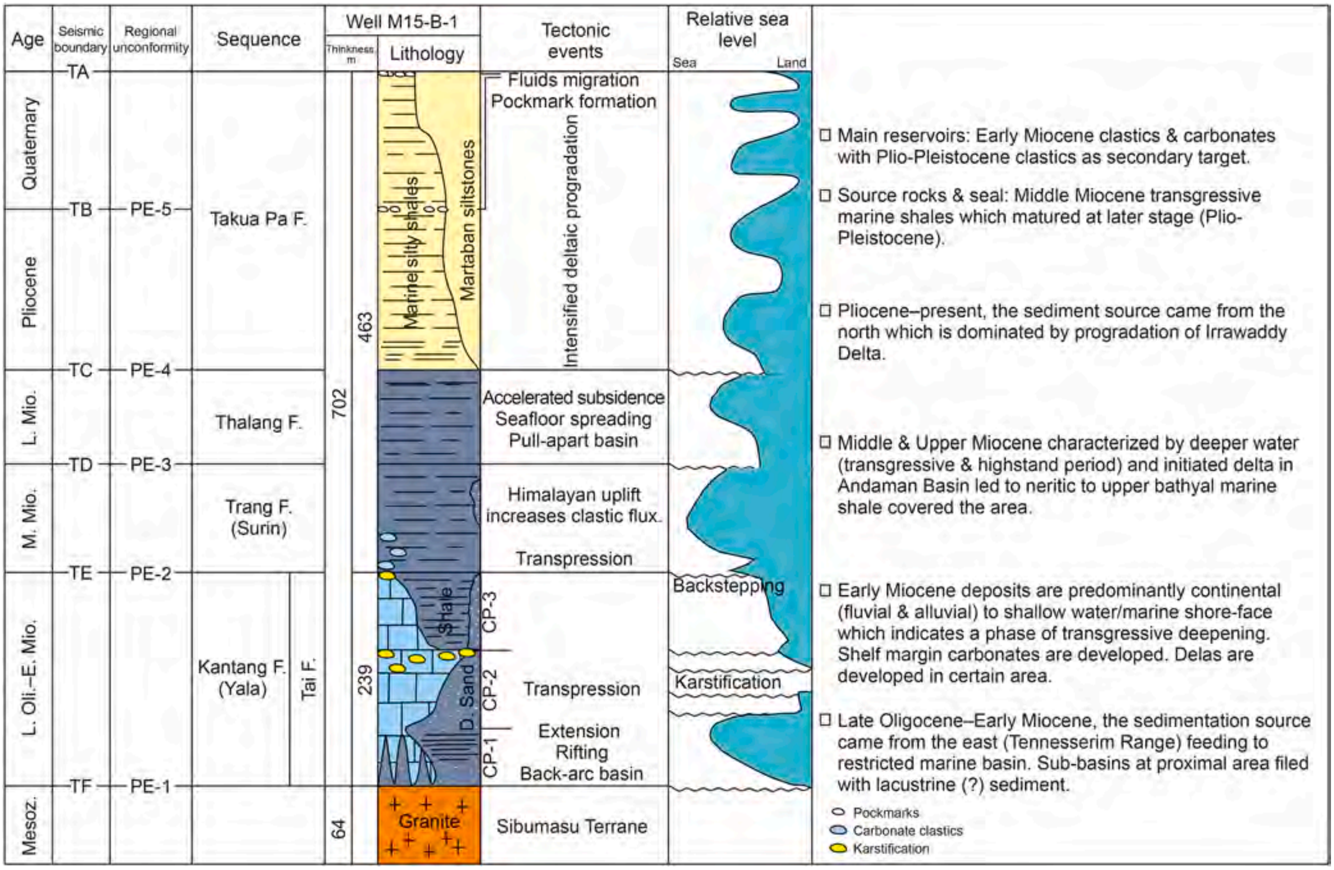

Fig. 2. Sequence stratigraphic framework of the study area, as controlled by the M15-B-1 exploration well synthesized from Bolton et al. (2013), Cao et al. (2015), Campbell et al. (2018), Jöhnck et al. (2020), Miller et al. (2020), Komar and Zeebe (2021), Mahattanachai et al. (2021), and Zhang et al. (2022). The stratigraphic architecture of the study area emphasizes major tectonostratigraphic transitions during Oligocene–Recent basin evolution. The figure highlights the phase of carbonate platform development approximately from Late Oligocene to Early Miocene in the Andaman Sea Basin under complex interactions among tectonic events and sea-level change.

depth, 564 channels, 12.5 m receiver interval). The recording system operated at a 2 ms sample rate, with a 2 Hz low-cut filter and 200 Hz high-cut filter, and a record length of 8192 ms. The final processed dataset for the block integrates both the 2016 and 2018 surveys, providing a comprehensive subsurface imaging framework for exploration and reservoir characterization (Fig. 3).

In addition to the 3D dataset, an extensive 2D seismic dataset covering 5100 km (Fig. 3), collected during three exploration programs from 1979 to 2004, was used. These 2D lines featured high-resolution parameters with 12.5 m channel spacing, 25 m gun spacing, and 2 ms sampling intervals. These data provide comprehensive coverage of the M-15 Block, effectively imaging major tectonic structures in various orientations, thereby establishing a solid framework for structural and stratigraphic analysis.

3.3. Methodology

This study employed an integrated analysis of 2D and 3D seismic reflection data (Fig. 3) to investigate the morphological evolution of the Tanintharyi Shelf carbonate platform and its implications for hydrocarbon reservoirs. The seismic data were processed and examined using the Petrel E&P® Software Platform. The approach began with a comprehensive review of existing literature to establish the regional geological context. Due to limited direct well control in the study area, the seismic stratigraphy was calibrated by incorporating data from exploration wells and published chronostratigraphic information from adjacent basins, specifically the Martaban and Mergui basins (Polachan and Racey, 1994; Racey and Ridd, 2015b; Morley, 2017; Raveendrasinghe et al., 2024) (Fig. 2).

Six key chronostratigraphic boundaries (TA to TF) were identified, enabling the mapping of five major seismic horizons ranging from the Quaternary to the Early Miocene periods. The interpretation of these horizons was carried out through a combination of automatic 3D tracking and manual refinement on a seismic grid with a spacing of 50 m × 50 m, extending from the seafloor to the basement. This process was further supported by data from the M15-B-1 exploration well. The horizons were then correlated with the region's established Cenozoic stratigraphy, facilitating the reconstruction of depositional sequences and environmental changes, especially sea-level fluctuations in the Andaman Sea Basin. Additionally, detailed seabed topography data were incorporated with subsurface seismic interpretations to map submarine geomorphological features and their relationships with underlying structures.

To clarify the internal architecture of the carbonate platform and the pathways of fluid migration, a set of seismic attributes was extracted and thoroughly analyzed. Root-mean-square (RMS) amplitude attributes were used to identify strong amplitude anomalies associated with significant unconformities and lithological contrasts (Chen and Sidney, 1997; Wang et al., 2025). Variance attributes were selectively filtered to improve the delineation of intervals mainly composed of carbonate lithologies and to detect structural discontinuities (Chen and Sidney, 1997; Wang et al., 2025). These attributes supported a spatial and temporal analysis of fault systems and features related to fluid

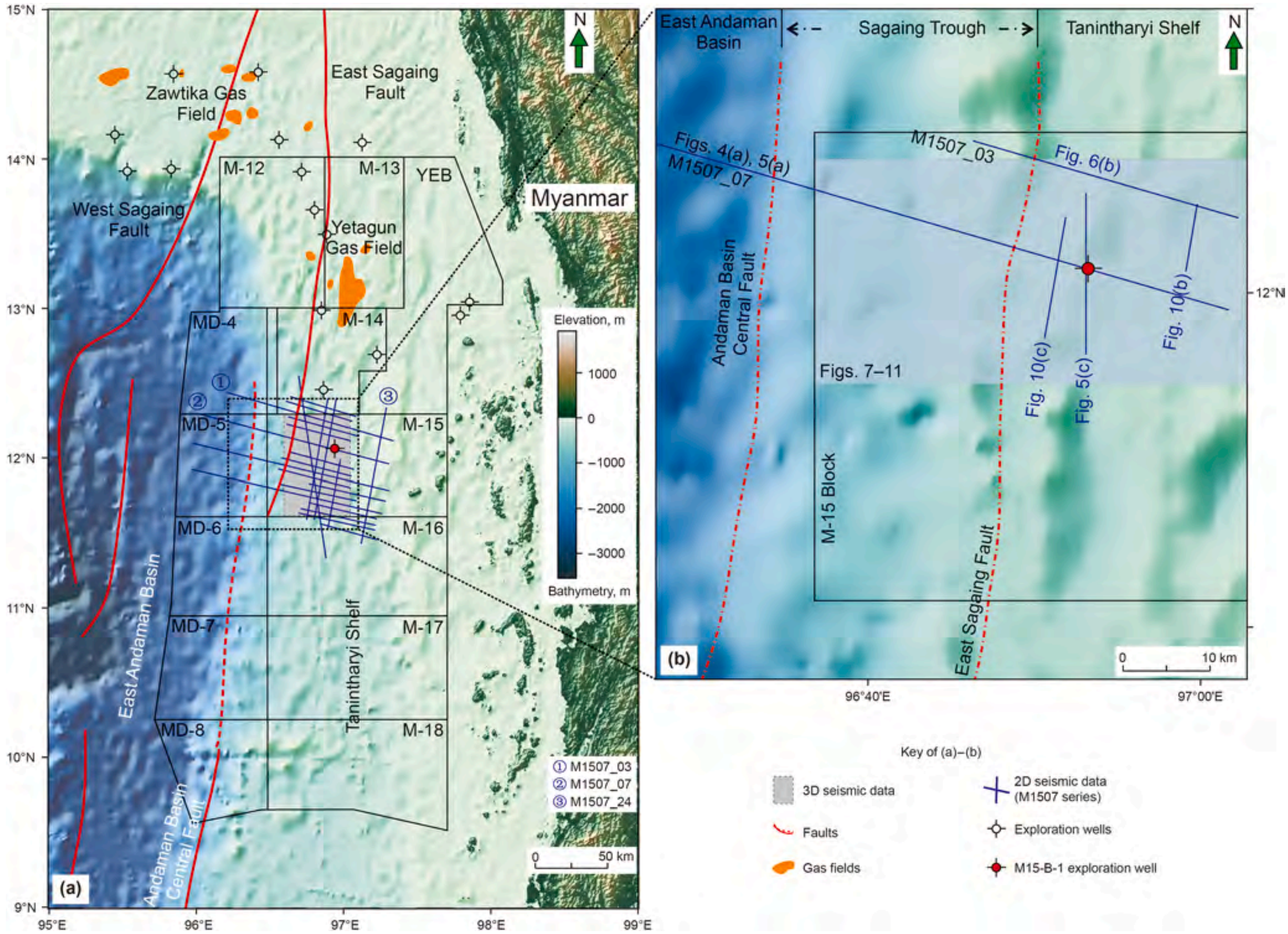

Fig. 3. **(a)** Seafloor map of the Tanintharyi Shelf and adjacent areas showing the distribution of 3D and 2D seismic survey lines within the study area, along with major faults and the locations of producing gas fields; **(b)** a detailed layout of the M-15 Block illustrating the spatial distribution of the interpreted seismic profiles discussed in this study, including the M15-B-1 exploratory well.

movement (Chen and Sidney, 1997; Lake and Srinivasan, 2004; Xue et al., 2024). Additionally, three-dimensional visualization techniques were employed to model sedimentary flow pathways and interpret the internal structure and relationships of seafloor features, including pockmarks and gas chimneys, in relation to the underlying strata.

The integration of seismic stratigraphy, attribute analysis, and geological indicators helped identify potential conduits for hydrocarbon migration, storage zones, and leakage features (Chen and Sidney, 1997; Xue et al., 2024; Wang et al., 2025). Edge detection analysis was used to show how tectonic activity affected reservoir architecture by visualizing the curvature of the platform. Ultimately, this comprehensive approach creates a tectonostratigraphic framework for the Tanintharyi Shelf, linking the interpreted fluid flow patterns and platform shape to Cenozoic tectonic events and eustatic changes to assess the potential for hydrocarbon accumulation.

4. Results

4.1. Stratigraphic framework of the Tanintharyi Shelf and its controls on carbonate platform development

The stratigraphic succession of the Tanintharyi Shelf overlies a Mesozoic crystalline basement, which is predominantly composed of granite and granodiorite gneiss (Racey and Ridd, 2015c; Morley, 2017). Notably, granitic units of the Sibumasu Terrane have been identified in the M15-B-1 well, providing a basement context for carbonate nucleation on structural highs (Fig. 2). Seismic sections define five main chronostratigraphic sequences (Late Oligocene–Early Miocene, Middle Miocene, Late Miocene, Pliocene, and Quaternary) (Figs. 2 and 4), each recording distinct tectono-sedimentary conditions that shaped the carbonate platform's evolutionary trajectory.

Direct evidence from the M15-B-1 exploration well, drilled near the 200 m isobath to investigate the Early Miocene carbonate platform, confirms the development of a shallow-marine carbonate system (Tai Formation) that is overlain by a thick siliciclastic cover—a key stratigraphic transition marking the platform's burial (Figs. 2 and 5). Well logs reveal a 64 m granitic basement interval of the Sibumasu Terrane, with a siliciclastic cover of approximately 463 m overlying the carbonate platform; the total Cenozoic succession above the Mesozoic basement reaches ~702 m, illustrating the juxtaposition of carbonate buildups on structural highs and clastic-dominated deposits in adjacent—a stratigraphic pattern that controlled the initial spatial distribution of carbonate precipitation (Figs. 2 and 5).

The lowermost Cenozoic interval (Upper Oligocene to Lower Miocene), bounded by the PE-1 and PE-2 unconformities and the TF–TE seismic boundaries (Figs. 2 and 4), forms the fundamental

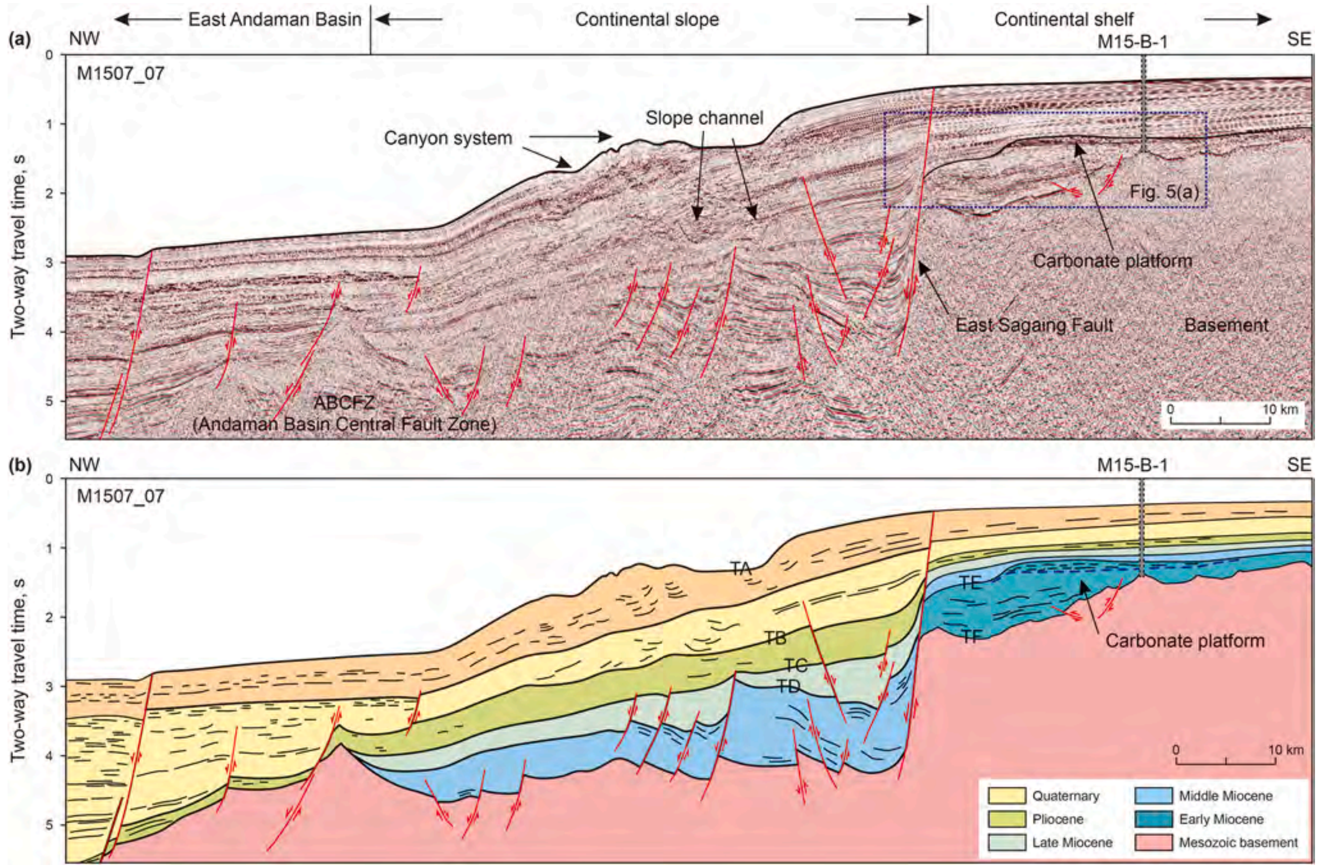

Fig. 4. (**a**) Uninterpreted and (**b**) interpreted M1507_07 seismic profile from the East Andaman Basin to the Tanintharyi Shelf (refer to Fig. 3 for detailed location information), illustrating the stratigraphic configuration with the carbonate platform along the shelf margin (Qiao et al., 2023; Jin et al., 2024; Raveendrasinghe et al., 2024).

stratigraphic foundation for carbonate platform initiation. This interval is characterized by deltaic sandstones lapping onto the eroded basement surface, with contemporaneous shallow-marine carbonates forming selectively on structural highs (Figs. 2 and 4). In the M15-B-1 stratigraphic section, the Early Miocene carbonate platform developed within this interval, enveloped by basal fanglomerate and fluvio-deltaic sandstones of the Kantang Formation, with local thin marine shale layers of the Yala Formation (~73 m thick) (Figs. 2 and 4). Subsequent tectono-sedimentary activity, particularly the transpressional episode during the Early Miocene, induced erosional modification and morphological fragmentation of the early platform, a stratigraphic response that influenced the platform's early growth pattern.

The Middle Miocene succession, demarcated by the PE-3 unconformity, consists primarily of shallow-marine shale (Trang Formation) with scattered deltaic sandstones (Surin Formation). This interval coincides with the transpressional tectonic regime on the Tanintharyi Shelf. The Late Miocene sequence, above the PE-3 unconformity, is dominated by marine silty shales with carbonaceous detritus and siltstones (Thalang Formation) (Figs. 2 and 4), recording accelerated basin subsidence linked to Andaman Sea seafloor spreading and a marked increase in siliciclastic flux—a stratigraphic change that directly triggered the drowning of the carbonate platform.

The Pliocene (TC–TB) and Quaternary (TB–TA) sequences, separated by the PE-5 unconformity, are composed of alternating marine silty shales and pro-deltaic Martaban siltstones (Takua Pa Formation) (Figs. 2 and 4) and represent the final stratigraphic stage of carbonate platform burial. This interval is characterized by intensified deltaic progradation, slope instability, chaotic seismic facies, submarine landslides, and canyon incision on the slope (Figs. 2 and 4), with widespread siliciclastic deposition completely smothering the residual carbonate platform and forming the regional cap rock over the carbonate reservoir system.

Seismic facies and thickness patterns across the shelf–basin transition exhibit a pronounced asymmetry (Figs. 5 and 6), driven by tectonic subsidence, eustatic sea-level fluctuations, and variable clastic input—all of which are encoded in the stratigraphic record and directly modulated carbonate platform morphology (Racey and Ridd, 2015c; Morley, 2017; Raveendrasinghe et al., 2024). Seismic reflections are parallel to subparallel and continuous across carbonate structural highs, reflecting stable shallow-marine conditions favorable for carbonate precipitation, while reflections become distorted, discontinuous, and thicken basinward, where shelf carbonates laterally pass into prograding deltaic and basin-fill siliciclastics (Figs. 5 and 6). Unconfirmed Late Oligocene strata beneath parts of the shelf and localized fan-shaped deposits east of the Mergui Ridge indicate a complex early depositional environment, with potential lacustrine or lacustrine-sourced facies analogs that may have influenced the initial paleotopography for carbonate nucleation (Raveendrasinghe et al., 2024).

Thus, the Tanintharyi Shelf's stratigraphic framework—defined by regional unconformities (PE-1 to PE-5), alternating carbonate and siliciclastic depositional environments, and sharp lateral facies changes (Figs. 2, 4 and 6)—not only provides the temporal and spatial context for carbonate platform evolution but also controls the distribution of diagenetic processes (e.g., potential dolomitization) and the quality of prospective Cenozoic carbonate reservoir units on the shelf and adjacent basinal depocenters.

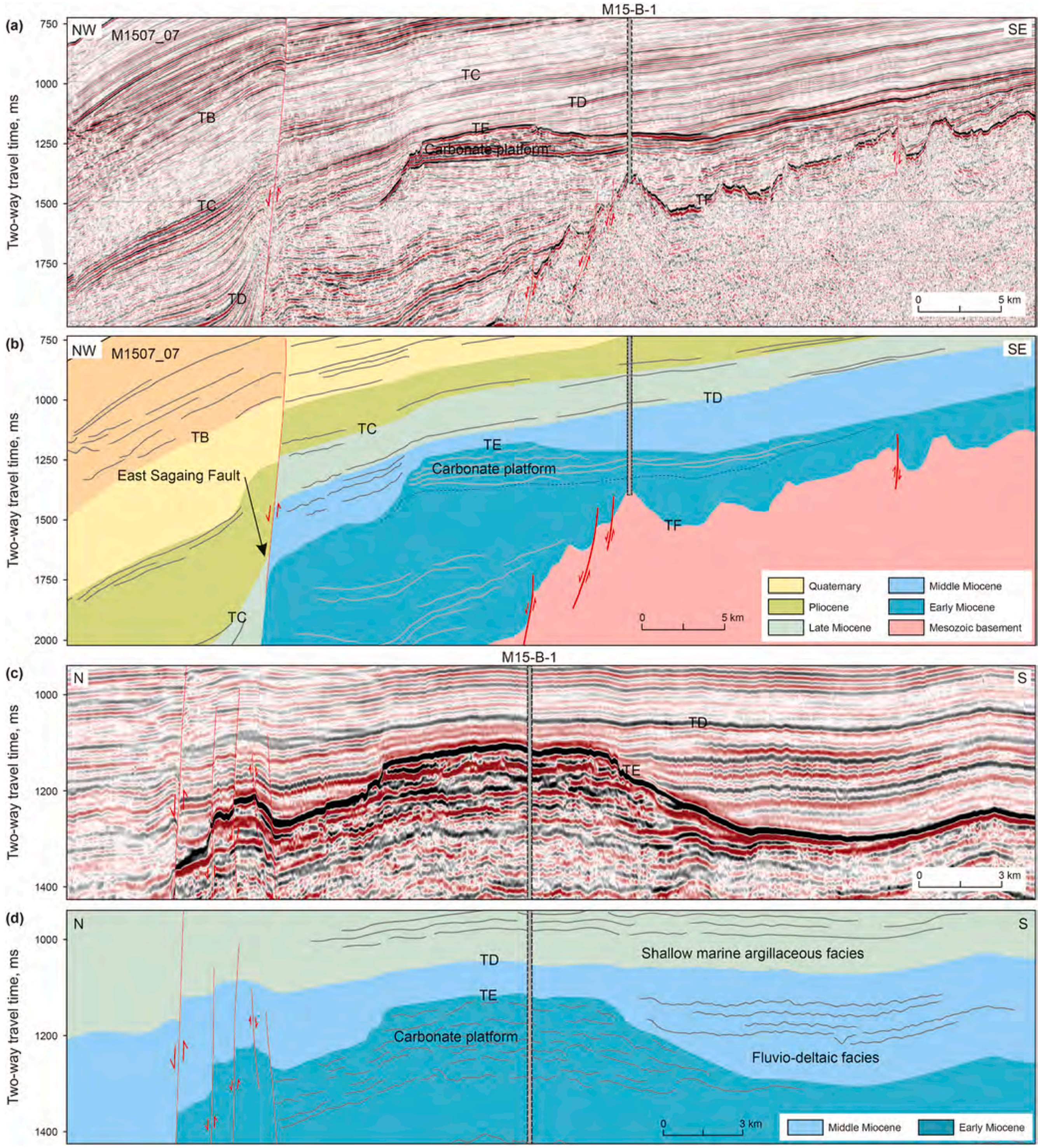

Fig. 5. (**a**) Uninterpreted and (**b**) interpreted M1507_07 seismic profile showing the carbonate platform developed on the shelf adjacent to the East Sagaing Fault. (**c**) Uninterpreted and (**d**) interpreted N–S trending seismic profile derived from the 3D seismic volume, illustrating the morphology of the carbonate platform buried beneath the fluvio-deltaic shelf stratigraphic configuration (refer to Fig. 3 for detailed location information).

4.2. Tectono-sedimentary setting and depositional environment of the carbonate platform

The Tanintharyi Shelf carbonate platform was predominantly developed during the Early Miocene rifting phase, constrained by the regional tectonic framework and depositional dynamics of the Andaman Sea Basin. It is spatially associated with an asymmetric synclinal structure that dips westward (Fig. 4), with sediment thickness maximizing along the axial depression and gradually thinning toward the eastern truncation margin (Fig. 7). This structural configuration was directly shaped by syn-rift faulting, which created favorable accommodation space for carbonate accumulation while isolating the shelf from excessive clastic influx (Raveendrasinghe et al., 2024).

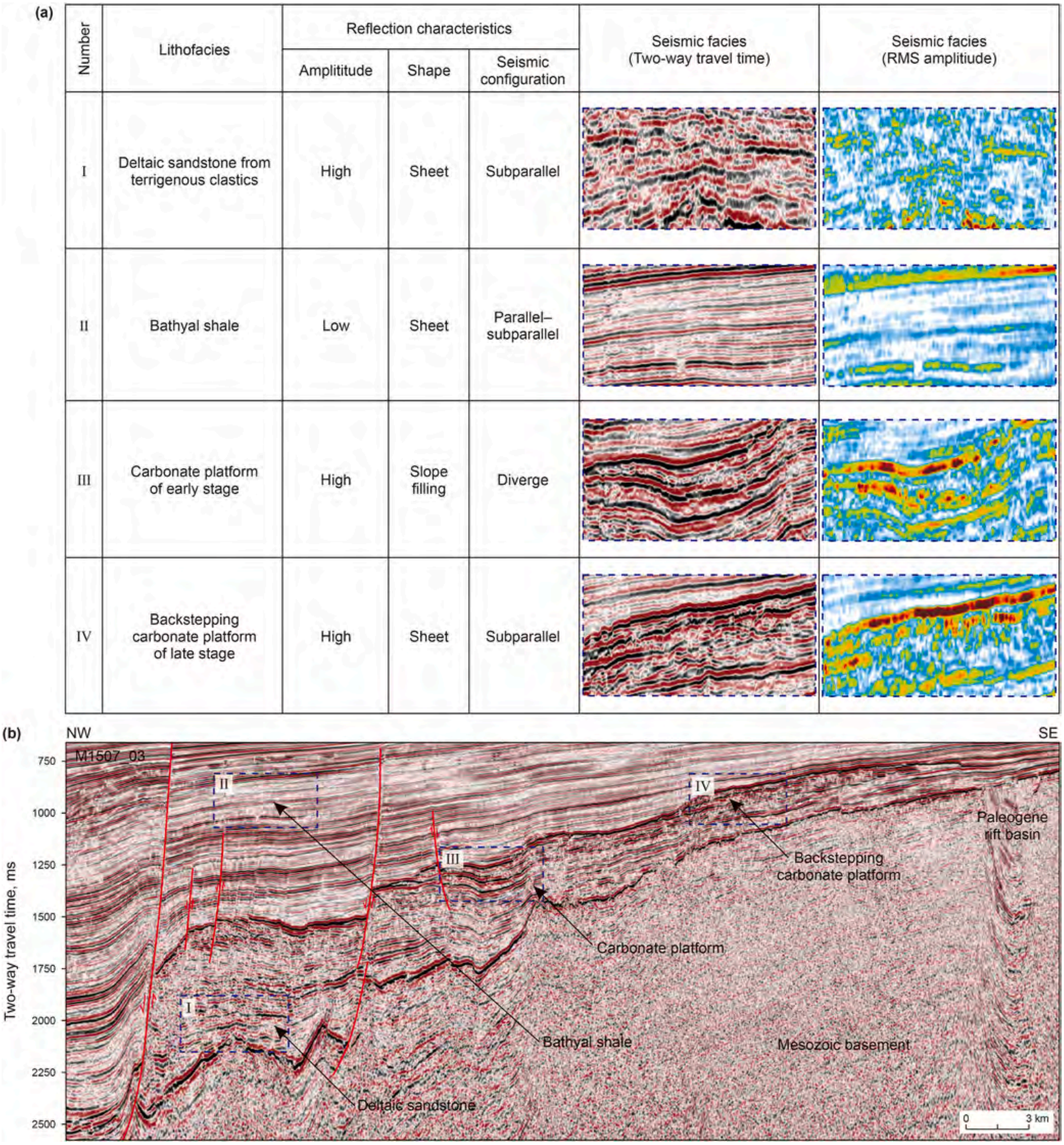

Fig. 6. **(a)** Summary of seismic reflection characteristics of the carbonate platform and surrounding lithofacies, based on amplitude, configuration, and internal geometry; **(b)** uninterpreted seismic section M1507_03 aligned in the NW–SE direction, displaying the spatial distribution of the carbonate platform underlain by the Mesozoic basement and flanked by deltaic sandstone deposits (refer to Fig. 3 for detailed location information).

Seismic profiles exhibit parallel to subparallel reflections arranged in continuous, mat-like patterns (Fig. 6), indicative of a stable, low-energy depositional environment where carbonate production was well-balanced with moderate tectonic subsidence. This depositional setting aligns with the characteristics of a rimmed carbonate shelf (Wilson, 1974; Bosence, 2005), where the platform margin was capable of sustaining wave-resistant facies while the inner shelf experienced calm hydrodynamic conditions.

3D seismic data further reveal fault-controlled depocenters adjacent to the platform (Fig. 7), which acted as sinks for localized clastic accumulation and prevented terrigenous material from encroaching on the carbonate-producing areas. Reflection strength displays a distinct proximal–distal gradient: stronger amplitudes near the platform edge correspond to coarse-grained bioclastic carbonates, while amplitudes weaken basinward toward the East Andaman Basin, reflecting a lateral transition to finer-grained outer-shelf sediments (Fig. 7).

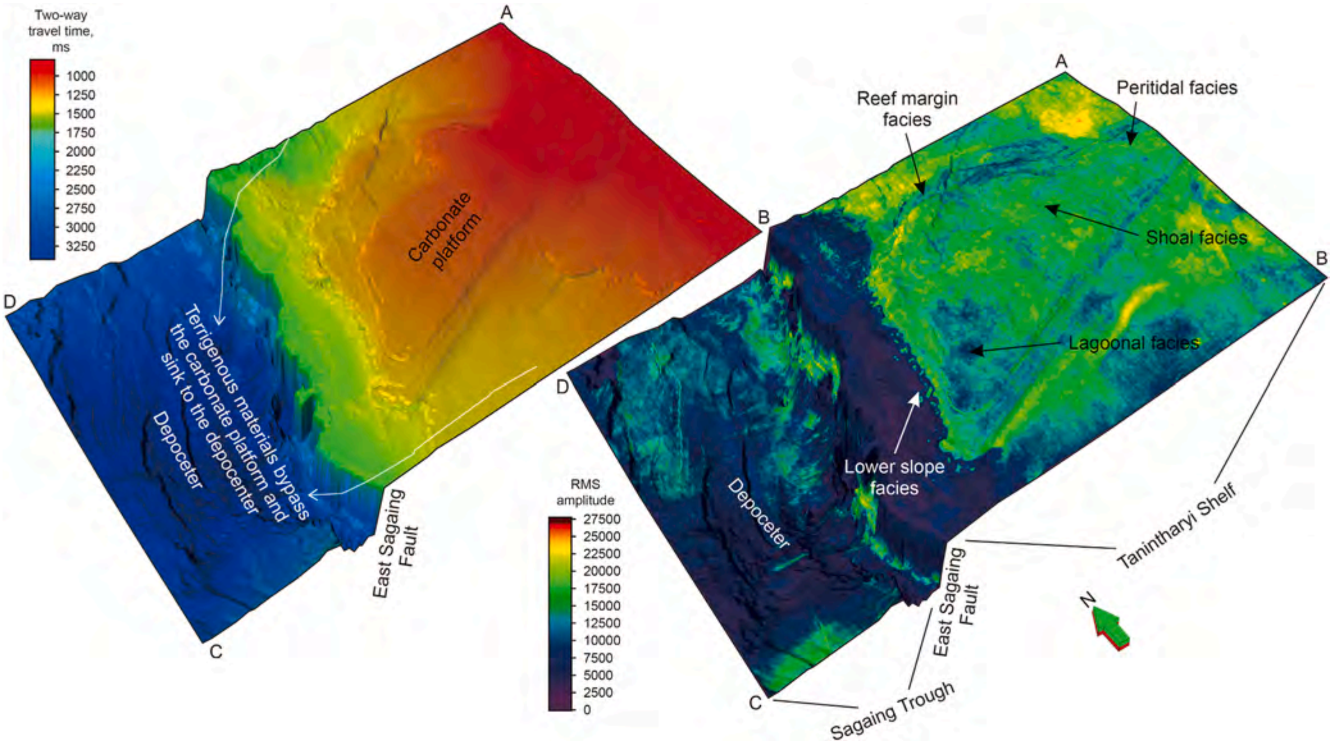

Fig. 7. Three-dimensional perspective of the morphology of the carbonate platform adjacent to the graben structure (Sagaing Trough), derived from a 3D seismic volume. The figure highlights the potential depositional facies associated with the carbonate platform and the bypass of the terrigenous materials to the depocenter, which does not disturb the carbonate platform, thereby maintaining it as a suitable environment for the carbonate development. The position of the East Sagaing Fault delineates the boundary between the Tanintharyi Shelf and the Sagaing Trough (refer to Fig. 3 for detailed location information).

The post-Early Miocene succession unconformably overlies the carbonate platform and grades upward into bioclastic-rich sediments and further into bathyal shales (Fig. 6). These strata exhibit parallel, high-continuity reflections typical of aggradational stacking under transgressive conditions, recording the progressive drowning and burial of the carbonate platform during the post-rift subsidence phase. This transition marks a fundamental shift in the basin's depositional regime, driven by accelerated tectonic subsidence and increased siliciclastic input—key factors that terminated carbonate production on the Tanintharyi Shelf.

4.3. Morphology and internal architecture of the carbonate platform

The internal lithofacies and morphological evolution of the Tanintharyi Shelf carbonate platform, interpreted from integrated 2D and high-resolution 3D seismic data surrounding the M15-B-1 well, reveal a distinct three-stage development during the Early Miocene, separated by two unconformities (Figs. 8 and 9). Variations in seismic reflection amplitude, continuity, and geometry document the dynamic adjustments of depositional environments in response to shifting tectonic and accommodation conditions.

4.3.1. Initiation stage (patch reef nucleation)

The platform's initiation is recorded in the basal carbonate unit (CP-1), characterized by weak, low-frequency reflections and low acoustic impedance contrast—indicative of fine-grained micritic deposition within fault-controlled depressions. Scattered mound-shaped features, ranging 100–300 m in width, are distributed atop thin clastic layers overlying the Mesozoic basement (Figs. 8 and 9). These mounds exhibit hummocky reflections and intermittent seismic blanking, signifying heterogeneous patch reefs interspersed with clastic interbeds. Notably, the mounds thicken basinward toward the southwest and onlap structural highs, indicating that they nucleated on fault-related paleotopography during the early syn-rift subsidence phase (Figs. 8 and 9). This morphology reflects localized carbonate deposition constrained by tectonically induced relief, amid ongoing clastic input from adjacent depocenters.

4.3.2. Development stage (platform formation)

The development stage is defined by a thick (400–600 ms TWT) composite platform unit (CP-2), characterized by continuous, medium-strong reflections of moderate frequency that replace the earlier mound geometries. This transition signifies the coalescence of isolated patch reefs into a continuous carbonate platform, with extensive algal and skeletal production on the original topography high at the steep western margin (>15°). Vertical aggradation and localized progradation shaped a distinct diamond platform morphology. Additionally, dolomitization features—likely driven by subaerial exposure—are focused along central highs and northern depressions, forming irregular, thicker zones interpreted as high-porosity dolomite bodies resistant to compaction. This morphological configuration establishes a clear proximal–distal facies gradient, with coarse-grained reefal carbonates dominating the margin and finer-grained outer-shelf sediments extending basinward (Figs. 8 and 9).

4.3.3. Extinction stage (exposure, karstification, and burial)

This final phase (CP-3) includes a resurgence of carbonate deposition along with the ongoing subsidence and transgression after the sea-level drop amid the Early Miocene (Fig. 2). The uppermost carbonate layer gradually thins landward (200–400 ms TWT) and exhibits heterogeneous seismic facies: chaotic, high-amplitude reflections in the northwest contrast with lower-

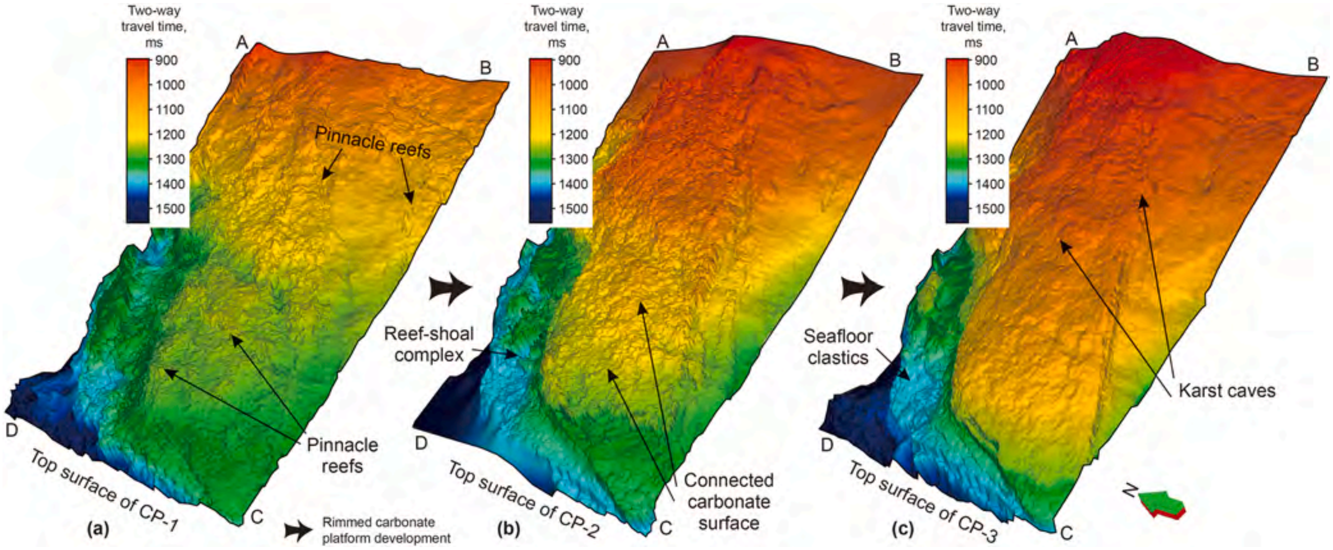

Fig. 8. Development stages of the carbonate platform (refer to Fig. 3 for detailed location information). **(a)** Top surface of CP-1 showing disseminated patch and pinnacle reef build-ups on the basement, representing the initial stage of the carbonate platform; **(b)** top surface of CP-2 illustrating the extensive development stage of the platform with a well-defined rimmed shape; **(c)** top surface of CP-3 displaying karst-related cavities, indicating the extinction stage of the platform.

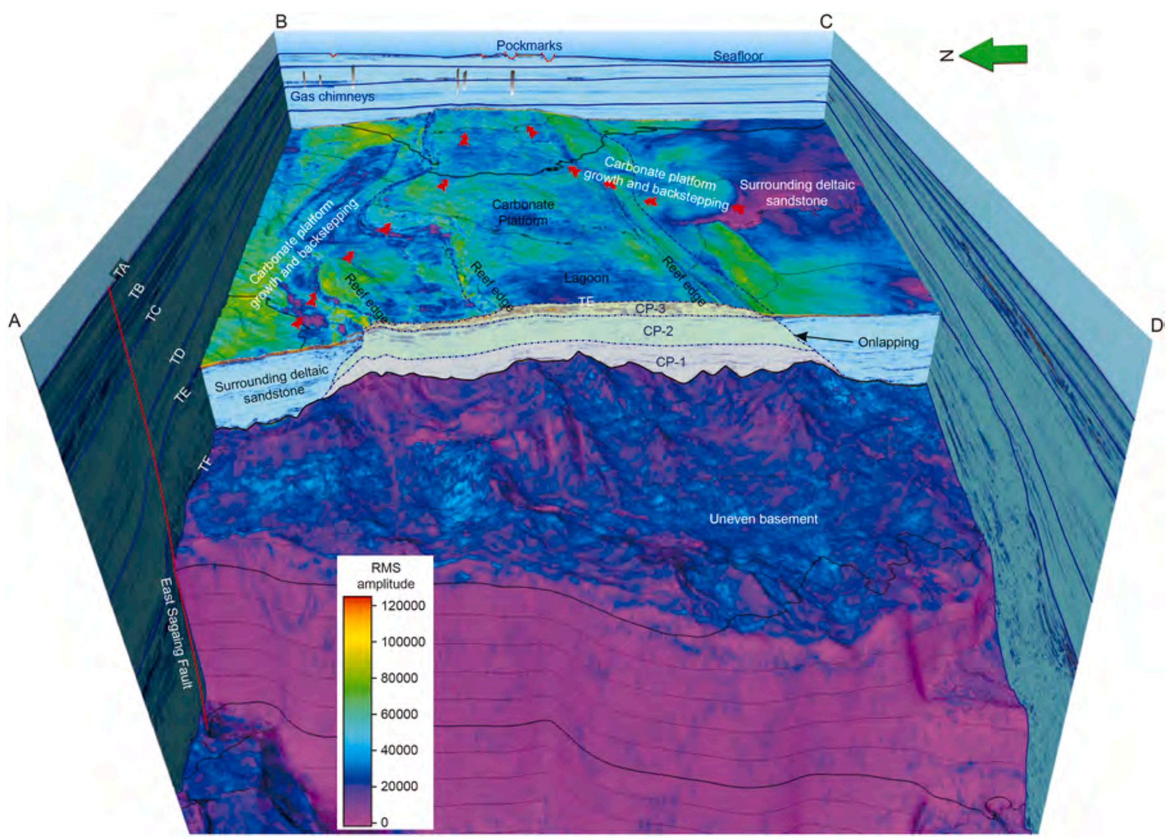

Fig. 9. Geological model derived using RMS seismic attributes, illustrating the uneven basement of the carbonate platform growth upon, and the relationship between the carbonate platform and the surrounding deltaic sandstones, and the backstepping trajectory as the carbonate platform growing upward. Gas chimneys and pockmarks also shown along the seismic section over the carbonate platform (refer to Fig. 3 for detailed location information).

amplitude, bioclastic-rich facies in the southeast (Figs. 8 and 9). A karstification interface is interpreted between CP-2 and CP-3 based on the sea-level drop during the CP-2 and CP-3 gap. The platform's extinction is marked by a prominent high-amplitude capping reflector with 20–50 m of relief, interpreted also as a karstified surface recording periods of subaerial exposure and initial submergence. Above this surface, weak-to medium-amplitude parallel reflections from the post-rift clastic succession onlap the carbonate margins, signifying a shift toward mixed siliciclastic deposition (Figs. 8 and 9).

Collectively, seismic stratigraphy documents the complete morphological evolution of the Tanintharyi Shelf carbonate platform—from fault-controlled patch reef initiation, to the formation of a diamond platform, and ultimately to exposure, karstification, and burial. This evolution reflects the combined influence of syn-rift faulting, sea-level fluctuations, and huge sediment input from Himalaya, resulting in a laterally and vertically heterogeneous, westward-dipping carbonate platform. Key morphological features, including marginal reef complexes and central dolomitized highs, have critical implications for the preservation and reservoir potential of the Early Miocene succession.

4.4. Pockmark trains, gas chimneys, and their constraints on carbonate platform morphology and hydrocarbon migration

Seismic interpretation of the Tanintharyi Shelf reveals widespread signs of subsurface fluid migration features, such as gas chimneys and pockmarks, formed above the carbonate platform (Figs. 9 and 10). The gas chimneys appear as vertical to nearly vertical zones of chaotic or disrupted reflections, usually extending upward from the carbonate platform into the overlying layers. These chimneys range from a few hundred meters to over 1 km in height, with diameters of 200–300 m, and often end within the Pleistocene to Recent shale layers. Their vertical continuity and high-amplitude chaotic internal reflections suggest that they are focused fluid channels connecting deep reservoirs to shallower sedimentary layers. Most gas chimneys are capped by acoustic blanking zones and subtle pull-down effects beneath the current seafloor, indicating localized gas-charged sediments or shallow fluid build-ups (Figs. 9 and 10).

Above these fluid pathways, distinct pockmark depressions are identified both within buried strata and on the modern seabed (Figs. 9 and 10). Paleo-pockmarks are primarily found within the Pliocene units, characterized by downward-tapering, concave “U”- to “V”-shaped geometries that truncate the underlying reflectors. In contrast, the present-day seabed features a well-developed, crescent-shaped pockmark train situated along the eastern geomorphologic high of the shelf. This pockmark train extends over 12 km in length, and ~2 km in width, with individual depressions reaching a depth of around 50 m and exhibiting steep-sided morphologies. The pockmark train delineates a belt of focused seepage along the structural margin of the carbonate platform (Fig. 11).

The height of gas chimneys and the distribution of the pockmark clusters within the strata indicate a two-stage process of fluid expulsion. The aggregation of pockmarks at the paleo-surface of the Pliocene, indicates the first stage of gas migration. A subsequent phase of renewed overpressure within the Pleistocene to Recent marine shale layer prompted reactivation of fluid flow along existing conduits, leading to the formation of the current seafloor pockmark pattern (Fig. 11). Although large-scale fault control is absent, minor fractures around the chimneys and local structural highs seem to have directed upward fluid movement from the carbonate platform.

5. Discussion

5.1. Evolution of the carbonate platform

The Tanintharyi Shelf in the Andaman Sea shows a progression from the formation and eventual decline of a large Cenozoic carbonate platform to later siliciclastic deposits (Figs. 2 and 9). The underlying Mesozoic basement relief and syn-sedimentary faulting (Qiao et al., 2023; Raveendrasinghe et al., 2024) provided localized space during the Late Oligocene, allowing deltaic sandstones to fill in structural lows while isolated shallow-marine carbonates started to form on uplifted highs. By the middle of the Early Miocene, initial carbonate buildups had connected into a more continuous platform, with sea-level changes and tectonic activity playing key roles in creating space for growth (Jöhnck et al., 2020; Miller et al., 2020) (Fig. 9).

Seismic and well data indicate that this platform developed as an asymmetric, west-tilted syncline, with consistent reef growth along the flanks of the structure high balanced by moderate subsidence along a central sag axis (Figs. 4 and 6). The early stage of platform formation featured small, mound-like reef structures forming on fault-bounded structure highs (Fig. 8). Seismic geomorphology shows a basal carbonate layer with weak, low-frequency reflections, interpreted as fine-grained micritic carbonates interlayered with thin clastic layers above the basement. In this period, isolated reef mounds, about 100–300 m wide, often thickened basinward and onlapped onto basement highs. These features suggest the carbonate platform started as patch reefs on structural highs during early syn-rift subsidence, reflecting localized carbonate deposition influenced by fault-related paleotopography amid ongoing clastic input (Racey and Ridd, 2015c; Morley, 2017) (Figs. 8 and 9).

As the reef development advanced, the reefs merged into a large, carbonate platform characterized by a consistent internal depositional pattern (Fig. 8). Seismic sections show a thick composite unit with continuous, moderate-amplitude reflections, indicating substantial algal and skeletal carbonate buildup (Hendry et al., 2021). The platform’s western side developed a steep edge made of wave-resistant reefal facies (Wilson, 1974; Hendry et al., 2021), while the eastern flank had a gentler slope (Figs. 8 and 9). This asymmetry created a clear proximal–distal facies gradient, with coarse-grained bioclastic carbonates dominating at the platform area and finer outer-shelf deposits extending outward area (Wilson, 1974). Vertical aggradation proceeded in tandem with the formation of accommodation space, and limited reef-edge shifting indicated a stable, upward-building carbonate platform under relatively low-energy conditions (Wilson, 1974; Hendry et al., 2021) (Figs. 8 and 9).

The end of the platform’s development was marked by a shift to exposure, erosion, and eventual drowning. A prominent unconformity at the top of the carbonate sequence, seen as a high-amplitude reflector with relief in seismic profiles, indicates subaerial exposure and karstification of the platform top surface (Figs. 5, 6 and 8). Later, sedimentation became increasingly dominated by siliciclastic materials (Morley, 2017; Raveendrasinghe et al., 2024): parallel, onlapping seismic reflections show deltaic and fluvial deposits that covered the carbonate platform (Racey and Ridd, 2015c; Qiao et al., 2023; Jin et al., 2024). During this period, the carbonate layer thinned landward and showed reduced continuity, with facies patterns becoming heterogeneous as isolated carbonate formations were preserved among the invading clastics (Qiao et al., 2023; Raveendrasinghe et al., 2024). This progressive infill by overlying marine silts and sands records the drowning and final burial of the Tanintharyi carbonate platform during post-rift subsidence (Figs. 5, 6, 8 and 9) (Morley, 2017; Raveendrasinghe et al., 2024).

Together, these facies and geomorphic trends illustrate the full life cycle of the Tanintharyi carbonate platform, primarily shaped by tectonic activity and sea-level changes (Wilson, 1974; Hendry et al., 2021) (Fig. 2). The asymmetric, shelf structure and documented proximal–distal zonation indicate prolonged buildup on structural highs (Figs. 5 and 9), while the bounding unconformities and onlapping clastics highlight phases of erosion and siliciclastic resurgence (Qiao et al., 2023; Jin et al., 2024; Raveendrasinghe et al., 2024). These combined observations offer a foundational

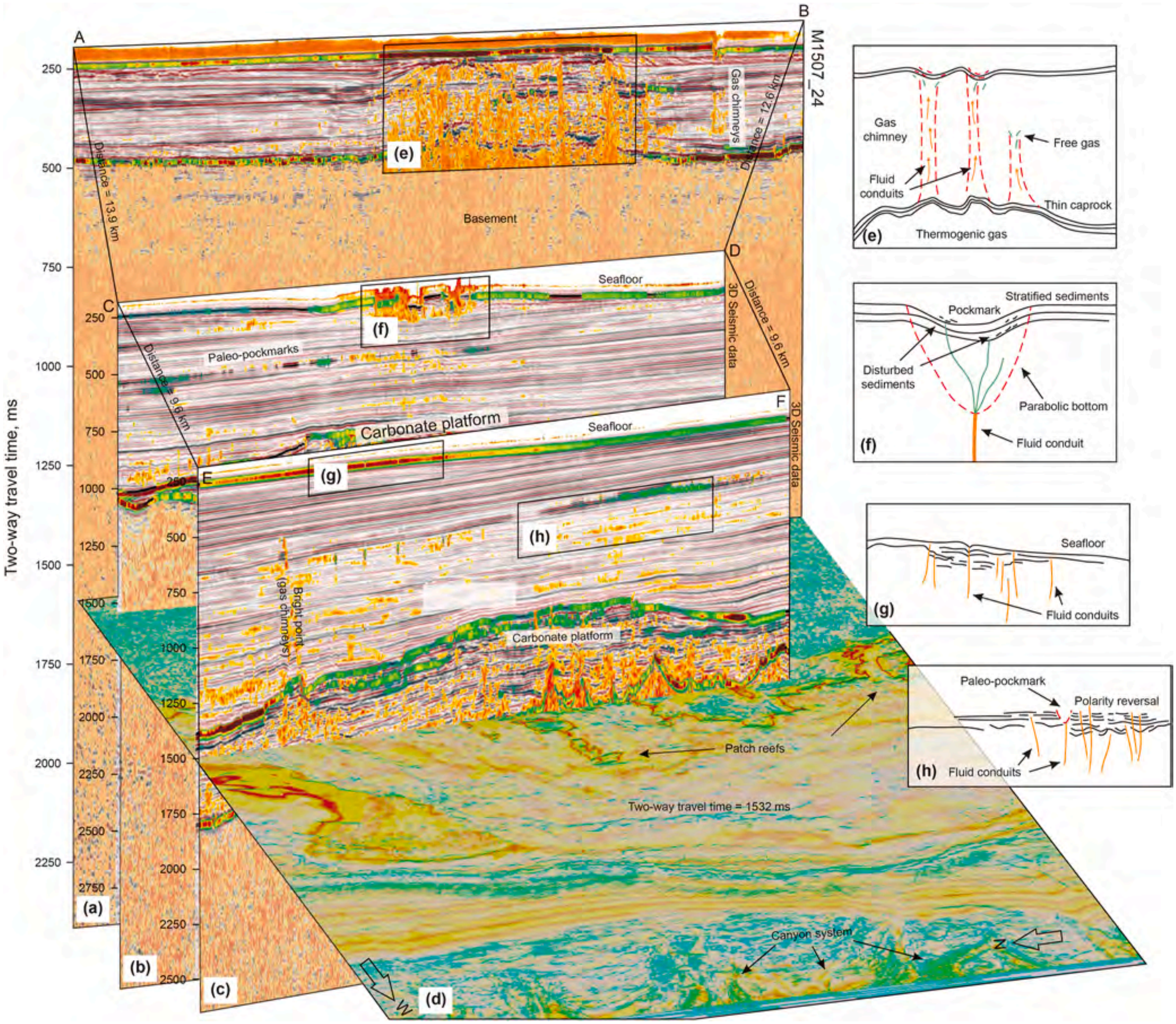

Fig. 10. Intersecting time-slice at 1532 ms and vertical seismic profiles illustrating the characteristic morphologies of fluid escape structures, including gas chimneys and pockmarks, within the sedimentary succession overlying the carbonate platform. The seismic sections display the spatial relationship between fluid conduits and the carbonate platform, highlighting the pathways and surface expressions of subsurface fluid migration (refer to Fig. 3 for detailed location information).

context for the detailed discussion of platform initiation, development, facies architecture, and drowning.

5.1.1. Influence of tectonic process

The Cenozoic tectonic evolution of the Andaman Sea, situated at the complex Indo-Eurasian plate boundary (Fig. 1), played a key role in shaping the morphological development of the Tanintharyi Shelf carbonate platform. Its initiation, architecture, and eventual demise were fundamentally governed by a dynamic tectonic regime that created and altered accommodation space, influenced paleotopography, and controlled sediment supply (Figs. 2 and 4). A crucial structural feature was the Andaman Basin Central Fault Zone (ABCFZ), which, during the Early Miocene, established a significant paleo-bathymetric divide (Mahattanachai et al., 2021; Raveendrasinghe et al., 2024) (Figs. 1 and 3). Subsidence of the East Andaman Basin along the ABCFZ resulted in a relatively uplifted margin to the east (Mahattanachai et al., 2021; Raveendrasinghe et al., 2024). This tectonic division was vital, as it isolates the shelf from deep water environment, which serves as a sink for terrigenous sediments, thereby creating conditions conducive to extensive carbonate accumulation and avoiding interference from terrigenous clastics (Burgess et al., 2013) (Fig. 7). Simultaneously, movement along the East Sagaing Fault Zone added further structural complexity, generating a series of graben and half-graben structures to the east of the ABCFZ (Raveendrasinghe et al., 2024) (Figs. 4 and 7). The Tanintharyi platform developed mainly on the relatively stable horst blocks and gentle shelf areas near these structures (Figs. 4 and 7), providing sustained accommodation space and directing siliciclastic sediments into the rapidly subsiding grabens to the west (Jin et al., 2024).

The initial syn-rift subsidence phase generated a mosaic of fault-bounded horsts and grabens (Morley, 2017; Mahattanachai et al., 2021) that directly influenced early platform morphology (Figs. 8 and 9). Uplifted fault blocks remained within the photic zone, serving as nucleation sites for patch reefs and bioclastic carbonate mounds, while intervening lows accumulated thin clastic sediments (Figs. 7 and 8). As carbonate development

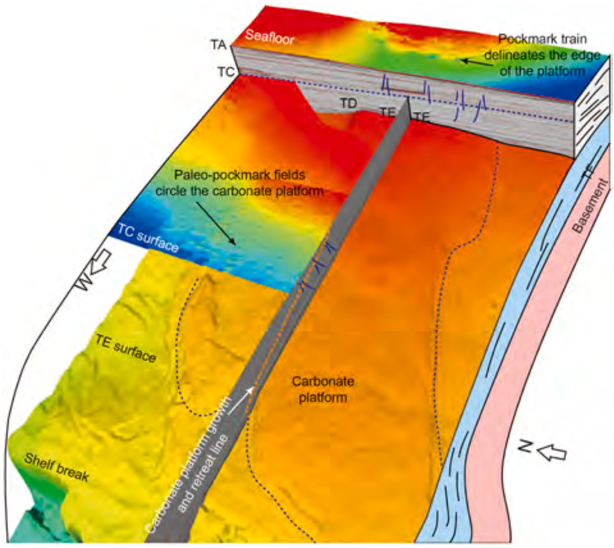

Fig. 11. Bathymetric of seafloor, TC surface, TE surface and seismic profiles depicting the backstepping of the carbonate platform edge and the pockmark fields surrounding the edge of the carbonate platform, as interpreted by Qiao et al. (2023) (refer to Fig. 3 for detailed location information).

continued, these isolated buildups merged into a continuous, carbonate platform occupying the whole horst. The NE–SW trending East Andaman Basin (Raveendrasinghe et al., 2024) further contributed to the platform's distinctive asymmetric, westward-dipping synclinal structure, with depocenters thickening basinward (e.g., westward) (Figs. 7 and 9). This structural framework established a clear proximal–distal facies gradient, as evidenced by seismic data. Coarse-grained reefal facies were present along the western margin, with finer outer-shelf deposits occurring distally to the west (Figs. 4 and 6). Intermittent transpressional pulses and uplift led to the development of key unconformities, some of which display karstification, indicating phases of platform exposure and subaerial erosion (Raveendrasinghe et al., 2024) (Fig. 8).

The platform's development was suddenly halted by a major tectonic reorganization after the Early Miocene, driven by intensified Indo-Eurasian collision (Fig. 2). The rifting and subsequent seafloor spreading in the Central Andaman Basin significantly restructured the regional physiography, constricting the Tanintharyi Shelf and increasing siliciclastic input from nearby uplifted terrains (Curray, 2005; Ramaswamy and Rao, 2014; Morley et al., 2022) (Figs. 1 and 2). This tectonic inversion, combined with the end of activity along the ABCFZ (Mahattanachai et al., 2021; Raveendrasinghe et al., 2024), stopped carbonate production and caused the platform to drown and become buried (Figs. 4 and 9). The following post-rift phase, marked by back-arc extension and strike-slip reorganization, enabled the progradation of deltaic systems that eventually smothered the carbonate factory (Curray, 2005; Morley, 2017; Morley et al., 2022). From a reservoir standpoint, these tectonic processes had two effects: first, they created the necessary structural framework for reservoir development, including paleo-highs, rimmed margins, and potential dolomitization zones in central highs; second, they established the stratigraphic pathways for its degradation and sealing through onlapping clastics and fault-related migration conduits (Fig. 9).

5.1.2. *Influence of sea-level fluctuations*

Sea-level change played a primary role in shaping the morphogenesis and stratigraphic architecture of the Tanintharyi Shelf carbonate platform (Fig. 2) by controlling the available space for carbonate buildup and pacing the cycles of aggradation, exposure, and backstepping recorded in seismic and well data. During the Late Oligocene–Early Miocene syn-rift period, rising sea levels, driven by regional subsidence and eustatic factors (Miller et al., 2020), created new accommodation on fault-bounded highs and enabled the formation of isolated patch reefs and mound-like structures (Figs. 8 and 9). When carbonate production locally met or surpassed accommodation, these nucleating structures merged into a rimmed shelf marked by continuous, parallel seismic reflections (Figs. 5, 8 and 9), indicating ongoing vertical accretion within the photic zone. Conversely, where accommodation exceeded production or where clastic supply increased, carbonate growth was limited, and facies became more diverse, resulting in the proximal–distal amplitude gradients observed across the platform (Figs. 4 and 6).

Intermittent relative sea-level drops during the early to middle part of the Early Miocene (Fig. 2) created clear sequence boundaries and a prominent high-amplitude capping reflector that indicates subaerial exposure and karst development on the platform top (Figs. 8 and 9). This exposed surface, with local relief of tens of meters, records meteoric dissolution, erosion, and the beginning of meteoric diagenesis that increased secondary porosity (Ott et al., 2023) and formed a regional sequence boundary. Later transgression restored shallow-marine conditions but typically limited renewed carbonate growth to the platform edges (Fig. 9), resulting in landward stepping and thinning of upper carbonate layers; in the seismic record, this behavior appears as backstepping geometries, chaotic high-amplitude reflections in stressed depositional areas, and onlap of fine-grained siliciclastics onto the eroded surface (Wilson, 1974; Burgess et al., 2013; Hendry et al., 2021) (Figs. 6 and 9). These stratigraphic patterns reflect how sensitive the carbonate factory is to minor sea-level changes when superimposed on a tectonically active shelf (Wilson, 1974; Hendry et al., 2021; Lunt, 2023).

The platform's final drowning and subsequent burial resulted from the combined effect of a major transgressive pulse and accelerated post-rift subsidence (Figs. 2 and 4), which together raised the relative sea level to rise faster than the carbonate factory could rebuild (Teillet et al., 2019, 2020; Lunt, 2023). As the photic zone was transgressed, onlapping clinoforms and prograding siliciclastic wedges gradually smothered carbonate production and created the thick post-platform siliciclastic cover documented in well M15-B-1 and seismic profiles (Racey and Ridd, 2015b, 2015c; Teillet et al., 2019, 2020). Importantly, the sea-level-driven cycle of aggradation, exposure, and drowning (Figs. 2 and 9) strongly imprinted reservoir heterogeneity: exposure and meteoric alteration locally increased secondary porosity and led to diagenetic facies formation (including dolomitized zones on central highs), while transgressive siliciclastic onlap and burial favored sealing and lateral isolation of reservoir bodies (Figs. 8 and 9). In sum, eustatic oscillations, working together with syn- and post-rift tectonics (Morley, 2017; Miller et al., 2020; Lunt, 2023), controlled the timing and spatial pattern of carbonate accumulation, the development of key sequence boundaries, and the preservation potential and connectivity of prospective reservoir facies on the Tanintharyi Shelf.

5.1.3. *Sedimentary and diagenetic responses to Tibetan Plateau uplift*

The progressive uplift of the Tibetan Plateau during the Neogene (Wang et al., 2014, 2017; Ding et al., 2022) significantly influenced the sedimentary dynamics and diagenetic evolution of the Tanintharyi Shelf carbonate platform. In response to the ongoing Indo-Eurasian collision (Fig. 1), this uplift not only restructured regional drainage systems but also changed atmospheric circulation patterns, profoundly affecting sediment supply, seawater chemistry, and diagenetic processes throughout the Andaman Sea Basin (Najman et al., 2022; Zhang et al., 2023; Fathima et al., 2025). During the Middle Miocene, the increased uplift of the plateau (Fig. 2) heightened the gradients of major river systems like the Irrawaddy and Salween, leading to more siliciclastic material entering the Andaman Sea (Awasthi and Ray, 2019; Jonell et al., 2022; Ma et al., 2024). This rising influx gradually shifted depositional environments from predominantly carbonate to mixed clastic–carbonate systems (Teillet et al., 2019, 2020; Lunt, 2023) (Figs. 2 and 4), resulting in the drowning of the Tanintharyi platform. The greater detrital input decreased water clarity and limited light penetration in shallow marine areas (Fathima et al., 2025), reducing biogenic carbonate production and encouraging deltaic progradation over the previously steady carbonate factory (Paumard et al., 2017; Teillet et al., 2019, 2020; Lunt, 2023).

Simultaneously, the uplift-driven climatic changes strengthened the South Asian monsoon system, boosting seasonal rainfall and freshwater flow into the Andaman Sea (Ray and Radhakrishna, 2021; Zhang et al., 2023; Fathima et al., 2025). This led to lower salinity levels and higher nutrient input, altering the geochemical balance of the surface ocean (Fathima et al., 2025). These conditions favored heterozoan over photozoan carbonate production and encouraged early diagenetic changes (Westphal et al., 2010; Teillet et al., 2019). This aligns with seismic and stratigraphic data showing widespread stacking patterns from aggradation to progradation, along with a shift from high-energy reef margin facies to fine-grained bioclastic- and siliciclastic-rich carbonates during the platform's late stage (Figs. 6 and 9). The uplift-enhanced monsoon also increased continental weathering, raising the levels of dissolved ions like Mg^{2+} and Si^{4+} in the basin (Yang et al., 2021; Fathima et al., 2025), likely promoting dolomitization and silica cementation within the platform's interior.

In the late Neogene, the ongoing uplift of the Tibetan Plateau enhanced topographic relief and increased erosion in the hinterland, leading to more sediment being delivered to the Andaman Basin (Zhang et al., 2023; Fathima et al., 2025) (Fig. 2). This period also saw a regional shift toward a high-subsidence regime associated with back-arc extension and seafloor spreading (Curray, 2005; Morley, 2017), which sped up the burial of carbonate successions beneath prograding deltaic and turbiditic sediments (Figs. 4 and 9). Episodic release of diagenetic fluids through fault-controlled conduits, as shown by gas chimneys and pockmarks above the carbonate platform (Fig. 10), may also be indirectly linked to overpressure build-up (Qiao et al., 2023) driven by rapid sediment loading and tectonic compression, both effects of continued plateau uplift.

Thus, the uplift of the Tibetan Plateau acted as a distal yet dominant geodynamic force shaping the Tanintharyi Shelf carbonate platform through three interconnected mechanisms: increased siliciclastic input and decreased carbonate productivity caused by intensified monsoon-driven erosion; altered diagenetic pathways linked to changes in hydrology and seawater chemistry; and greater burial and compaction resulting from faster sedimentation and tectonic subsidence. These combined effects transformed the Tanintharyi platform from a lively Early Miocene carbonate system into a mixed carbonate–siliciclastic shelf and eventually into a buried reservoir complex with intricate diagenetic fabrics and diverse porosity. The stratigraphic and seismic records of this transformation thus record a sedimentary and diagenetic history of the far-reaching influence of Tibetan Plateau uplift on the evolving tectono-sedimentary framework of the Andaman Sea Basin (Zhang et al., 2023).

5.2. Implications for the prospective carbonate reservoir

The Early Miocene carbonate platform on the Tanintharyi Shelf is a highly promising yet naturally diverse reservoir system (Fig. 10). Seismic and well data show a rimmed-shelf structure mainly made up of wave-resistant reefal and algal grainstone facies along the western edge, which gradually transitions basinward into finer bioclastic- and siliciclastic-influenced carbonates (Figs. 7 and 9). This proximal–distal facies zoning creates predictable primary reservoir zones on structural highs but is characterized by rapid lateral and vertical facies changes that disrupt reservoir continuity (Joshi and Singh, 2019; Garland et al., 2025).

Diagenetic processes have greatly shaped this primary facies framework, creating a complex mosaic of preserved and destroyed porosity (Fig. 7). A pronounced high-amplitude unconformity at the top of the carbonate succession marks episodes of exposure and karstification, which locally produced secondary porosity (vuggy and moldic fabrics) within reef cores (Fig. 8). Additionally, intermittent early dolomitization in central highs and paleoreefs has resulted in the formation of dolomite bodies that are resistant to compaction and capable of maintaining favorable pore networks (Teillet et al., 2019, 2020) (Fig. 8). Conversely, ongoing burial under Late Miocene to Pliocene siliciclastics has possibly caused compaction and extensive carbonate cementation in deeper, basinward zones, leading to tightly cemented, low-quality rock. The overall result is a patchwork pore system where high-quality reefal and dolomitized cores are interspersed with cemented, mud-rich, and siliciclastic-influenced intervals, producing a porosity distribution that is highly discontinuous and closely linked to the timing and location of exposure, karstification, and subsequent burial (Jardine and Wilshart, 1987; Harris and Vlaswinkel, 2008; Hendry et al., 2021).

Seismic evidence shows widespread vertical fluid pathways, indicated by vertical gas chimneys and both buried and current seafloor pockmarks (Fig. 10). This suggests that the platform has served as both a transmission route for deeper hydrocarbons and a kitchen source. The two-stage fluid escape history observed, comprising an initial pulse in the Late Miocene and renewed activity in the Quaternary, indicates that the system has been in a saturated charge stage since at least the Late Miocene (Qiao et al., 2023) (Fig. 10). The extensive marine shales from the Middle Miocene to Pliocene act as an effective regional cap in many areas. However, local seal thinning and fault or fracture corridors have enabled leakage and focused seepage in certain locations, requiring an evaluation of chimney proximity and seal integrity on a case-by-case basis when assessing trap preservation.

From an exploration and appraisal perspective, the most promising targets are the reefal margin facies and potential dolomitized cores located on paleo-highs, where primary porosity has been enhanced by meteoric alteration and where dolomite has preserved pore networks from subsequent compaction (Jardine and Wilshart, 1987; Harris and Vlaswinkel, 2008; Hendry et al., 2021) (Fig. 7). Therefore, successful targeting requires high-resolution mapping of facies boundaries, sequence stratigraphic surfaces, and diagenetic bodies, all integrated with seismic-attribute analysis and correlated with available well control (as observed in M15-B-1) (Ghon et al., 2018) (Fig. 7). The main risks come from internal compartmentalization (such as intrabuild-up mudstones and sequence boundaries), variable cementation, and locally compromised seals related to chimneys and faulting (Harris and Vlaswinkel, 2008; Hendry et al., 2021). As a result, predictive models should incorporate fault architecture and subsidence history with sequence stratigraphy and diagenetic mapping to identify preserved porosity, evaluate both lateral and vertical connectivity, and assess seal integrity before development (Ghon et al., 2018). Once these factors are clarified, the Tanintharyi carbonate complex shows significant hydrocarbon potential, but only through workflows capable of addressing its depositional complexity and diagenetic influences.

6. Conclusions

This study provides a detailed analysis of the morphological evolution of the Tanintharyi Shelf carbonate platform in the Andaman Sea, integrating high-resolution seismic geomorphology, well data, and regional stratigraphy to develop a comprehensive tectono-sedimentary model with direct implications for Cenozoic hydrocarbon exploration. The main conclusions are as follows:

1) The Tanintharyi Shelf carbonate platform initiated in the late Oligocene to Early Miocene as isolated patch reefs on fault-bounded structural highs. It evolved into a westward-dipping, asymmetric rimmed shelf with a steep western margin and a gentler eastern flank. Its decline happened due to subaerial exposure, karstification, and eventual burial under prograding siliciclastic sediments during the Middle to Late Miocene, driven by accelerated post-rift subsidence.
2) The platform's initiation and extinction were influenced by three main factors: (1) Syn-sedimentary faulting created paleotopography and controlled accommodation space, enabling carbonate production while preventing siliciclastic influx. However, post-Early Miocene tectonic activity halted this growth and caused burial. (2) Changes in relative sea level triggered cycles of aggradation, backstepping, and exposure, with a major transgressive pulse eventually submerging the carbonate-producing areas. (3) The Neogene uplift of the Tibetan Plateau increased siliciclastic sediment supply and changed basin hydrochemistry through the intensification of the Asian monsoon, which suppressed carbonate productivity and promoted dolomitization.
3) The Tanintharyi Shelf carbonate platform is a complex and heterogeneous reservoir system. Primary reservoir quality appears in wave-resistant reefal and algal grainstone facies at the platform margin. Diagenetic processes like karstification have enhanced secondary porosity in structural highs, possibly forming dolomite bodies. However, high-quality zones are interspersed with tightly cemented intervals and mud-rich facies, causing significant compartmentalization. Widespread gas chimneys and pockmarks indicate the platform functions as both a reservoir and a pathway for fluid migration. Paleo- and current seafloor pockmarks suggest hydrocarbon charging in the carbonate platform. Although the overlying Miocene–Pliocene marine shales serve as an effective seal, individual traps may be compromised by fault and fracture corridors associated with fluid escape.

Thus, this research establishes a predictive tectonostratigraphic framework for the Tanintharyi Shelf, focusing on high-resolution mapping of facies boundaries, sequence stratigraphic surfaces, and diagenetic features, especially reef margins and potential dolomitization on paleo-highs. Consequently, hydrocarbon exploration should incorporate seal integrity and fault architecture, while also considering tectonic history along with eustatic and diagenetic models to forecast the distribution and quality of complex carbonate reservoirs in tectonically active, rift-margin settings worldwide.

CRediT authorship contribution statement

Xi-Wu Luan: Writing – review & editing, Supervision, Software, Resources, Project administration, Investigation, Funding acquisition, Data curation, Conceptualization, Formal analysis, Methodology, Validation, Visualization, Writing – original draft. **Thanuja D. Raveendrasinghe:** Writing – review & editing, Writing – original draft, Methodology, Investigation, Conceptualization, Data curation, Visualization. **Zi-Jie Wang:** Writing – review & editing, Writing – original draft, Visualization, Methodology, Investigation, Data curation. **Li-Shuang Feng:** Visualization, Writing – review & editing.

Declaration of competing interest

The authors declare that they have no known competing financial interests or personal relationships that could have appeared to influence the work reported in this paper.

Acknowledgements

This study is supported by the China-ASEAN Maritime Cooperation Fund Project (No. 12120100500017001) and the National Natural Science Foundation of China (Nos. 42249801, 92055211).

References

Awasthi, N., Ray, J.S., 2019. The Palaeogene record of Himalayan erosion in the Andaman Basin. J. Earth Syst. Sci. 129, 15. https://doi.org/10.1007/s12040-019-1266-7.
Bashir, Y., Faisal, M.A., Biswas, A., Babasafari, A.A., Ali, S.H., Imran, Q.S., Siddiqui, N.A., Ehsan, M., 2021. Seismic expression of Miocene carbonate platform and reservoir characterization through geophysical approach: application in central Luconia, offshore Malaysia. J. Pet. Explor. Prod. Technol. 11 (4), 1533–1544. https://doi.org/10.1007/s13202-021-01132-2.
Bolton, C.T., Chang, L., Clemens, S.C., Kodama, K., Ikehara, M., Medina-Elizalde, M., Paterson, G.A., Roberts, A.P., Rohling, E.J., Yamamoto, Y., Zhao, X., 2013. A 500,000 year record of Indian summer monsoon dynamics recorded by eastern equatorial Indian Ocean upper water-column structure. Quat. Sci. Rev. 77, 167–180. https://doi.org/10.1016/j.quascirev.2013.07.031.
Bosence, D.W., 2005. A genetic classification of carbonate platforms based on their basinal and tectonic settings in the Cenozoic. Sediment. Geol. 175 (1–4), 49–72. https://doi.org/10.1016/j.sedgeo.2004.12.030.
Burgess, P.M., Winefield, P., Minzoni, M., Elders, C., 2013. Methods for identification of isolated carbonate buildups from seismic reflection data. AAPG (Am. Assoc. Pet. Geol.) Bull. 97 (7), 1071–1098. https://doi.org/10.1306/12051212011.
Cao, P., Shi, X., Li, W., Liu, S., Yao, Z., Hu, L., Khokiattiwong, S., Kornkanitnan, N., 2015. Sedimentary responses to the Indian Summer Monsoon variations recorded in the southeastern Andaman Sea slope since 26 ka. J. Asian Earth Sci. 114, 512–525. https://doi.org/10.1016/j.jseaes.2015.06.028.
Campbell, S.M., Moucha, R., Derry, L.A., Raymo, M.E., 2018. Effects of dynamic topography on the Cenozoic carbonate compensation depth. G-cubed 19 (4), 1025–1034. https://doi.org/10.1002/2017gc007386.
Chatterjee, S., Goswami, A., Scotese, C.R., 2013. The longest voyage: tectonic, magmatic, and paleoclimatic evolution of the Indian plate during its northward flight from Gondwana to Asia. Gondwana Res. 23 (1), 238–267. https://doi.org/10.1016/j.gr.2012.07.001.
Chen, Q., Sidney, S., 1997. Seismic attribute technology for reservoir forecasting and monitoring. Lead. Edge 16 (5), 445–448. https://doi.org/10.1190/1.1437657.
Curray, J.R., 2005. Tectonics and history of the Andaman Sea region. J. Asian Earth Sci. 25 (1), 187–232. https://doi.org/10.1016/j.jseaes.2004.09.001.
Ding, L., Kapp, P., Cai, F., Garzione, C.N., Xiong, Z., Wang, H., Wang, C., 2022. Timing and mechanisms of Tibetan Plateau uplift. Nat. Rev. Earth Environ. 3 (10), 652–667. https://doi.org/10.1038/s43017-022-00318-4.
Fathima, R., Saraswat, R., Bhadra, S.R., Naik, D.K., Suokhrie, T., 2025. A strong influence of the precession and northern high latitudinal climate on the monsoon seasonality and productivity in the Andaman Sea. Global Planet. Change 254, 105017. https://doi.org/10.1016/j.gloplacha.2025.105017.
Gardiner, N.J., Searle, M.P., Morley, C.K., Robb, L.J., Whitehouse, M.J., Roberts, N.M., Kirkland, C.L., Spencer, C.J., 2018. The crustal architecture of Myanmar imaged through zircon U–Pb, Lu–Hf and O isotopes: Tectonic and metallogenic implications. Gondwana Res. 62, 27–60. https://doi.org/10.1016/j.gr.2018.02.008.
Garland, J., Barnett, A.J., Burchette, T., Wright, V.P., 2025. An introduction to 'Carbonate Reservoirs: Applying Current Knowledge to Future Energy Needs'. Geol. Soc., London, Spec. Publ. 548 (1), 1–11. https://doi.org/10.1144/sp548-2024-117.
Ghon, G., Rankey, E., Baechle, G., Schlaich, M., Ali, S., Mokhtar, S., Poppelreiter, M., 2018. Carbonate Reservoir Characterisation of an Isolated Platform Integrating Sequence Stratigraphy and Rock Physics in Central Luconia. Conference Proceedings, 80th EAGE Conference and Exhibition 2018. Jun 2018, pp. 1–5. https://doi.org/10.3997/2214-4609.201800800.
Guo, M., Luan, X., Zhang, H., He, B., 2023. Geometric and kinematic analysis of faults bordering the Andaman Sea continental shelves: a 3D seismic case

study. Front. Earth Sci. 11, 1247665. https://doi.org/10.3389/feart.2023.1247665.
Hall, R., 2012. Late Jurassic–Cenozoic reconstructions of the Indonesian region and the Indian Ocean. Tectonophysics 570–571, 1–41. https://doi.org/10.1016/j.tecto.2012.04.021.
Harris, P.M., Vlaswinkel, B., 2008. Modern Isolated carbonate platforms: Templates for quantifying facies attributes of hydrocarbon reservoirs. In: Lukasik, J., Simo, J.A. (Eds.), Controls on Carbonate Platform and Reef Development. SEPM Special Publication, vol. 89, pp. 323–341. https://doi.org/10.2110/pec.08.89.0323.
Hendry, J., Burgess, P., Hunt, D., Janson, X., Zampetti, V., 2021. Seismic characterization of carbonate platforms and reservoirs: An introduction and review. Geol. Soc., London, Spec. Publ. 509, 1–28. https://doi.org/10.1144/sp509-2021-51.
Henglai, P., Fongngern, R., Saller, A., 2024. The growth and demise of a Middle Miocene carbonate platform in Central Luconia, offshore Malaysia. Mar. Petrol. Geol. 163, 106763. https://doi.org/10.1016/j.marpetgeo.2024.106763.
Jardine, D., Wilshart, J.W., 1987. Carbonate reservoir description. In: Tillman, R.W., Weber, K.J. (Eds.), Reservoir Sedimentology. SEMP Special Publication, vol. 40, pp. 129–152. https://doi.org/10.2110/pec.87.40.0129.
Jin, L., Luan, X., Raveendrasinghe, T.D., Jiang, L., Xue, Y., Wei, X., Qiao, J., Ma, H., 2024. Influence of sedimentary processes and fault tectonics on the evolution of submarine canyons in the East Andaman Basin: Insights from high-resolution seismic data analysis. Geomorphology 454, 109179. https://doi.org/10.1016/j.geomorph.2024.109179.
Jithin, A.K., Francis, P.A., 2020. Role of internal tide mixing in keeping the deep Andaman Sea warmer than the Bay of Bengal. Sci. Rep. 10, 11982. https://doi.org/10.1038/s41598-020-68708-6.
Jöhnck, J., Kuhnt, W., Holbourn, A., Andersen, N., 2020. Variability of the Indian monsoon in the Andaman Sea across the Miocene–Pliocene transition. Paleoceanogr. Paleoclimatol. 35, e2020PA003923. https://doi.org/10.1029/2020pa003923.
Jonell, T.N., Giosan, L., Clift, P.D., Carter, A., Bretschneider, L., Hathorne, E.C., Barbarano, M., Garzanti, E., Vezzoli, G., Naing, T., 2022. No modern Irrawaddy River until the late Miocene–Pliocene. Earth Planet Sci. Lett. 584, 117516. https://doi.org/10.1016/j.epsl.2022.117516.
Joshi, R.M., Singh, K.H., 2019. Carbonate reservoirs: recent large to giant carbonate discoveries around the world and how they are shaping the carbonate reservoir landscape. In: Singh, K.H., Joshi, R.M. (Eds.), Petro-Physics and Rock Physics of Carbonate Reservoirs: Likely Elucidations and Way Forward. Springer, pp. 3–14. https://doi.org/10.1007/978-981-13-1211-3_1.
Khan, P., Chakraborty, P.P., 2004. Two-phase opening of Andaman Sea: A new seismotectonic insight. Earth Planet Sci. Lett. 229 (3–4), 259–271. https://doi.org/10.1016/j.epsl.2004.11.010.
Komar, N., Zeebe, R.E., 2021. Reconciling atmospheric CO_2, weathering, and calcite compensation depth across the Cenozoic. Sci. Adv. 7 (4), eabd4876. https://doi.org/10.1126/sciadv.abd4876.
Lake, L.W., Srinivasan, S., 2004. Statistical scale-up of reservoir properties: Concepts and applications. J. Petrol. Sci. Eng. 44 (1–2), 27–39. https://doi.org/10.1016/j.petrol.2004.02.003.
Lü, C., Wu, S., Yao, Y., Fulthorpe, C.S., 2013. Development and controlling factors of Miocene carbonate platform in the Nam Con Son Basin, southwestern South China Sea. Mar. Petrol. Geol. 45, 55–68. https://doi.org/10.1016/j.marpetgeo.2013.04.014.
Lunt, P., 2023. Biological evolution of Southeast Asian carbonates, based on their microfossil content. In: Rankey, E.C., Pöppelreiter, M.C. (Eds.), Cenozoic Isolated Carbonate Platforms—Focus Southeast Asia. SEPM Special Publication, vol. 114, pp. 70–84. https://doi.org/10.2110/sepmsp.114.07.
Ma, H., Luan, X., Raveendrasinghe, T.D., Wei, X., He, H., Qiao, J., Jin, L., Fan, G., Lu, Y., 2024. Tectonic influence on the evolutionary dynamics of deep-water channel systems along the active accretionary prism margin in the Rakhine Basin, Myanmar: A high-resolution 3D seismic analysis. Geomorphology 458, 109263. https://doi.org/10.1016/j.geomorph.2024.109263.
Mahattanachai, T., Morley, C.K., Charusiri, P., Kanjanapayont, P., 2021. The Andaman Basin Central Fault Zone, Andaman Sea: Characteristics of a major deepwater strike-slip fault system in a polyphase rift. Mar. Petrol. Geol. 128, 104997. https://doi.org/10.1016/j.marpetgeo.2021.104997.
Mathew, M., Makhankova, A., Menier, D., Sautter, B., Betzler, C., Pierson, B., 2020. The emergence of Miocene reefs in South China Sea and its resilient adaptability under varying eustatic, climatic and oceanographic conditions. Sci. Rep. 10, 7141. https://doi.org/10.1038/s41598-020-64119-9.
Miller, K.G., Browning, J.V., Schmelz, W.J., Kopp, R.E., Mountain, G.S., Wright, J.D., 2020. Cenozoic sea-level and cryospheric evolution from deep-sea geochemical and continental margin records. Sci. Adv. 6 (20), eaaz1346. https://doi.org/10.1126/sciadv.aaz1346.
Moeremans, R., Singh, S.C., 2015. Fore-arc basin deformation in the Andaman-Nicobar segment of the Sumatra-Andaman subduction zone: Insight from high-resolution seismic reflection data. Tectonics 34 (8), 1736–1750. https://doi.org/10.1002/2015tc003901.
Morley, C.K., 2017. Chapter 4 Cenozoic rifting, passive margin development and strike-slip faulting in the Andaman Sea: A discussion of established v. new tectonic models. Geol. Soc., London, Mem.. 47, 27–50. https://doi.org/10.1144/m47.4.
Morley, C.K., Alvey, A., 2015. Is spreading prolonged, episodic or incipient in the Andaman Sea? Evidence from deepwater sedimentation. J. Asian Earth Sci. 98, 446–456. https://doi.org/10.1016/j.jseaes.2014.11.033.
Morley, C.K., Chantraprasert, S., Chenoll, K., Sootlek, P., Jitmahantakul, S., 2022. Interaction of thin-skinned detached faults and basement-involved strike-slip faults on a transform margin: The Moattama Basin, Myanmar. Geol. Soc., London, Spec. Publ. 524, 165–190. https://doi.org/10.1144/sp524-2021-90.
Morley, C., Chantraprasert, S., Kongchum, J., Chenoll, K., 2021. The West Burma Terrane, a review of recent paleo-latitude data, its geological implications and constraints. Earth Sci. Rev. 220, 103722. https://doi.org/10.1016/j.earscirev.2021.103722.
Najman, Y., Sobel, E.R., Millar, I.L., Luan, X., Zapata, S., Garzanti, E., Parra, M., Vezzoli, G., Zhang, P., Aung, D.W., Paw, S.M.T.L., Lwin, T.S., 2022. The timing of collision between Asia and the West Burma Terrane, and the development of the indo-burman ranges. Tectonics 41, e2021TC007057. https://doi.org/10.1029/2021tc007057.
Ott, R., Gallen, S.F., Helman, D., 2023. Erosion and weathering in carbonate regions reveal climatic and tectonic drivers of carbonate landscape evolution. Earth Surf. Dyn. 11 (2), 247–257. https://doi.org/10.5194/esurf-11-247-2023.
Paumard, V., Zuckmeyer, E., Boichard, R., Jorry, S.J., Bourget, J., Borgomano, J., Maurin, T., Ferry, J., 2017. Evolution of late Oligocene–Early Miocene attached and isolated carbonate platforms in a volcanic ridge context (Maldives type), Yadana field, offshore Myanmar. Mar. Petrol. Geol. 81, 361–387. https://doi.org/10.1016/j.marpetgeo.2016.12.012.
Polachan, S., Racey, A., 1994. Stratigraphy of the Mergui Basin, Andaman Sea: Implications for petroleum exploration. J. Petrol. Geol. 17 (4), 373–406. https://doi.org/10.1111/j.1747-5457.1994.tb00147.x.
Qiao, J., Luan, X., Raveendrasinghe, T.D., Lu, Y., Fan, G., Wei, X., Jin, L., Yin, J., Ma, H., Jiang, L., 2023. Unravelling Cenozoic carbonate platform fluid expulsion: Deciphering pockmark morphologies and genesis in the Tanintharyi shelf of the Andaman Sea as promising hydrocarbon reservoirs. Mar. Petrol. Geol. 160, 106603. https://doi.org/10.1016/j.marpetgeo.2023.106603.
Racey, A., Ridd, M.F., 2015a. Chapter 6 Myanmar offshore petroleum overview. Geol. Soc., London, Mem.. 45, 57–62. https://doi.org/10.1144/m45.06.
Racey, A., Ridd, M.F., 2015b. Chapter 7 Petroleum geology of the Moattama Region, Myanmar. Geol. Soc., London, Mem.. 45, 63–81. https://doi.org/10.1144/m45.07.
Racey, A., Ridd, M.F., 2015c. Chapter 8 Petroleum Geology of the Tanintharyi Region, Myanmar. Geol. Soc., London, Mem.. 45, 83–91. https://doi.org/10.1144/m45.08.
Raju, K.A.K., Ramprasad, T., Rao, P.R.V., Rao, B.D., Varghese, J.R., 2004. New insights into the tectonic evolution of the Andaman Basin, northeast Indian Ocean. Earth Planet Sci. Lett. 221 (1–4), 145–162. https://doi.org/10.1016/s0012-821x(04)00075-5.
Ramaswamy, V., Rao, P.R.V., 2014. Chapter 17 the Myanmar continental shelf. Geol. Soc., London, Mem.. 41, 231–240. https://doi.org/10.1144/m41.17.
Rankey, E.C., 2023. Deep-time perspectives on Miocene isolated carbonate platforms of Southeast Asia. In: Rankey, E.C., Pöppelreiter, M.C. (Eds.), Cenozoic Isolated Carbonate Platforms—Focus Southeast Asia. SEPM Special Publication, vol. 114, pp. 5–31. https://doi.org/10.2110/sepmsp.114.01.
Raveendrasinghe, T.D., Luan, X., Qiao, J., Jin, L., Wang, Z., Vikum, A., Xue, Y., Ma, H., Yang, R., Fan, G., Lu, Y., 2024. Unveiling the transtensional geodynamics of Cenozoic depocenter changes in the Andaman Sea: Seismic evidence for the existence of the East Sagaing Fault and the Andaman Basin Central Fault Zone in the Tanintharyi region. Mar. Petrol. Geol. 164, 106814. https://doi.org/10.1016/j.marpetgeo.2024.106814.
Ray, J.S., Radhakrishna, M., 2021. The Andaman Islands and Adjoining Offshore: Geology, Tectonics, and Palaeoclimate. Springer. https://doi.org/10.1007/978-3-030-39843-9.
Singh, S.C., Moeremans, R., 2017. Chapter 13 Anatomy of the Andaman–Nicobar subduction system from seismic reflection data. Geological Society, London, Memoirs, 47, 193–204. https://doi.org/10.1144/m47.13.
Srisuriyon, K., Morley, C.K., 2014. Pull-apart development at overlapping fault tips: Oblique rifting of a Cenozoic continental margin, northern Mergui Basin, Andaman Sea. Geosphere 10 (1), 80–106. https://doi.org/10.1130/ges00926.1.
Srivastava, D.K., Dave, A., Dangwal, V., 2021. Sequence stratigraphy of the Andaman Basin, northern Indian Ocean. Mar. Petrol. Geol. 133, 105298. https://doi.org/10.1016/j.marpetgeo.2021.105298.
Teillet, T., Fournier, F., Gisquet, F., Montaggioni, L.F., Borgomano, J., Villeneuve, Q., Hong, F., 2019. Diagenetic history and porosity evolution of an Early Miocene carbonate buildup (Upper Burman Limestone), Yadana gas field, offshore Myanmar. Mar. Petrol. Geol. 109, 589–606. https://doi.org/10.1016/j.marpetgeo.2019.06.044.
Teillet, T., Fournier, F., Montaggioni, L.F., BouDagher-Fadel, M.K., Borgomano, J., Braga, J.C., Villeneuve, Q., Hong, F., 2020. Development patterns of an isolated oligo-mesophotic carbonate buildup, early Miocene, Yadana field, offshore Myanmar. Mar. Petrol. Geol. 111, 440–460. https://doi.org/10.1016/j.marpetgeo.2019.08.039.
Wang, G., Cao, K., Wang, A., Shen, T., Zhang, K., Wang, L., 2014. On the geodynamic mechanism of episodic uplift of the Tibetan Plateau during the Cenozoic Era. Acta Geol. Sin. Engl. Ed. 88 (2), 699–716. https://doi.org/10.1111/1755-6724.12223.
Wang, W., Zheng, W., Zhang, P., Li, Q., Kirby, E., Yuan, D., Zheng, D., Liu, C., Wang, Z., Zhang, H., Pang, J., 2017. Expansion of the Tibetan Plateau during the Neogene. Nat. Commun. 8 (1), 15887. https://doi.org/10.1038/ncomms15887.
Wang, Z., Luan, X., Raveendrasinghe, T.D., Jin, L., Wang, Y., Ma, H., Wang, J., 2025. The influence of Cenozoic fluid expulsion on the seafloor morphology of the Vulcan Sub-basin, northwest Australia: Implications of gas chimneys and linear diapirs for hydrocarbon exploration. Mar. Petrol. Geol. 180, 107481. https://doi.org/10.1016/j.marpetgeo.2025.107481.

Westphal, H., Halfar, J., Freiwald, A., 2010. Heterozoan carbonates in subtropical to tropical settings in the present and past. Int. J. Earth Sci. 99 (S1), 153–169. https://doi.org/10.1007/s00531-010-0563-9.

Wilson, J.L., 1974. Characteristics of carbonate-platform margins. AAPG (Am. Assoc. Pet. Geol.) Bull. 58 (5), 810–824. https://doi.org/10.1306/83d9149d-16c7-11d7-8645000102c1865d.

Xu, J., Ben-Avraham, Z., Kelty, T., Yu, H., 2014. Origin of marginal basins of the NW Pacific and their plate tectonic reconstructions. Earth Sci. Rev. 130, 154–196. https://doi.org/10.1016/j.earscirev.2013.10.002.

Xue, Y., Luan, X., Raveendrasinghe, T.D., Wei, X., Jin, L., Yin, J., Qiao, J., 2024. Implications of salt tectonics on hydrocarbon ascent in the eastern Persian Gulf: Insights into the formation mechanism of salt diapirs, gas chimneys, and their sedimentary interactions. J. Ocean Univ. China 23 (6), 1515–1533. https://doi.org/10.1007/s11802-024-5821-8.

Yang, Y., Ye, C., Galy, A., Fang, X., Xue, Y., Liu, Y., Yang, R., Zhang, R., Han, W., Zhang, W., Ruan, X., 2021. Monsoon-enhanced silicate weathering as a new atmospheric CO_2 consumption mechanism contributing to fast late Miocene global cooling. Paleoceanogr. Palaeoclimatol. 36, e2020PA004008. https://doi.org/10.1029/2020PA004008.

Zhang, H., Luo, Y., Yu, J., Zhang, L., Xiang, R., Yu, Z., Huang, H., 2022. Indian Ocean sedimentary calcium carbonate distribution and its implications for the glacial deep ocean circulation. Quat. Sci. Rev. 284, 107490. https://doi.org/10.1016/j.quascirev.2022.107490.

Zhang, P., Jiang, S., Li, R., Mei, L., 2023. Tectonic and climate forcing of exhumation in the SE Tibetan Plateau over the past 7 ma: insights from the deltaic-submarine fan system in the Andaman Sea, northeastern Indian Ocean. Palaeogeogr. Palaeoclimatol. Palaeoecol. 620, 111573. https://doi.org/10.1016/j.palaeo.2023.111573.